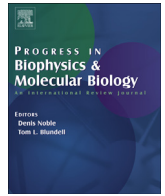




Contents lists available at ScienceDirect

## Progress in Biophysics and Molecular Biology

journal homepage: [www.elsevier.com/locate/pbiomolbio](http://www.elsevier.com/locate/pbiomolbio)

## The protective effect of ursodeoxycholic acid in an *in vitro* model of the human fetal heart occurs via targeting cardiac fibroblasts

Francisca Schultz<sup>a, b</sup>, Alveera Hasan<sup>a</sup>, Anita Alvarez-Laviada<sup>a</sup>, Michele Miragoli<sup>a, c</sup>, Navneet Bhogal<sup>a</sup>, Sarah Wells<sup>a</sup>, Claire Poulet<sup>a</sup>, Jenny Chambers<sup>b, d</sup>, Catherine Williamson<sup>b, d</sup>, Julia Gorelik<sup>a, \*</sup>

<sup>a</sup> National Heart and Lung Institute, Imperial Centre for Translational and Experimental Medicine, Imperial College London, London, UK

<sup>b</sup> Institute of Reproductive and Developmental Biology, Imperial College London, London, UK

<sup>c</sup> Humanitas Clinical and Research Institute, Rozzano, Italy

<sup>d</sup> Women's Health Academic Centre, King's College London, London, United Kingdom

## ARTICLE INFO

## Article history:

Received 15 September 2015

Received in revised form

5 January 2016

Accepted 6 January 2016

Available online xxx

## Keywords:

Fetal arrhythmia

Ursodeoxycholic acid

Fibroblasts

Bile acids

ATP-Dependent potassium channel

Fetal heart

## ABSTRACT

Bile acids are elevated in the blood of women with intrahepatic cholestasis of pregnancy (ICP) and this may lead to fetal arrhythmia, fetal hypoxia and potentially fetal death *in utero*. The bile acid taurocholic acid (TC) causes abnormal calcium dynamics and contraction in neonatal rat cardiomyocytes. Ursodeoxycholic acid (UDCA), a drug clinically used to treat ICP, prevents adverse effects of TC. During development, the fetus is in a state of relative hypoxia. Although this is essential for the development of the heart and vasculature, resident fibroblasts can transiently differentiate into myofibroblasts and form gap junctions with cardiomyocytes *in vitro*, resulting in cardiomyocyte depolarization. We expanded on previously published work using an *in vitro* hypoxia model to investigate the differentiation of human fetal fibroblasts into myofibroblasts.

Recent evidence shows that potassium channels are involved in maintaining the membrane potential of ventricular fibroblasts and that ATP-dependent potassium ( $K_{ATP}$ ) channel subunits are expressed in cultured fibroblasts.  $K_{ATP}$  channels are a valuable target as they are thought to have a cardioprotective role during ischaemic and hypoxic conditions. We investigated whether UDCA could modulate fibroblast membrane potential.

We established the isolation and culture of human fetal cardiomyocytes and fibroblasts to investigate the effect of hypoxia, TC and UDCA on human fetal cardiac cells.

UDCA hyperpolarized myofibroblasts and prevented TC-induced depolarisation, possibly through the activation of  $K_{ATP}$  channels that are expressed in cultured fibroblasts. Also, similar to the rat model, UDCA can counteract TC-induced calcium abnormalities in human fetal cultures of cardiomyocytes and myofibroblasts. Under normoxic conditions, we found a higher number of myofibroblasts in cultures derived from human fetal hearts compared to cells isolated from neonatal rat hearts, indicating a possible increased number of myofibroblasts in human fetal hearts. Hypoxia further increased the number of human fetal and rat neonatal myofibroblasts. However, chronically administered UDCA reduced the number of myofibroblasts and prevented hypoxia-induced depolarisation.

In conclusion, our results show that the protective effect of UDCA involves both the reduction of fibroblast differentiation into myofibroblasts, and hyperpolarisation of myofibroblasts, most likely

**Abbreviations:**  $\alpha$ SMA,  $\alpha$ -Smooth Muscle Actin; bpm, beats per minute; CM, cardiomyocyte; FB, fibroblast; ICP, Intrahepatic Cholestasis of Pregnancy; HBSS, Hanks' balanced salt solution;  $K_{ATP}$ , ATP-dependent potassium channel; Kir, potassium inward rectifier current; M199, medium 199; NCS, neonatal calf serum; P1075, N-cyano-N'-(1,1-dimethylpropyl)-N''-3-pyridylguanidine; RMP, resting membrane potential; SEM, standard error of the mean; SICM, Scanning Ion Conductance Microscopy; SUR, sulphonylurea receptor; TC, taurocholic acid; TCDA, taurochenodeoxycholic acid; UDCA, Ursodeoxycholic acid.

\* Corresponding author. National Heart and Lung Institute, Imperial Centre for Translational and Experimental Medicine, Imperial College London, London W12 0NN, UK.

E-mail address: [j.gorelik@imperial.ac.uk](mailto:j.gorelik@imperial.ac.uk) (J. Gorelik).

<http://dx.doi.org/10.1016/j.pbiomolbio.2016.01.003>  
0079-6107/© 2016 Published by Elsevier Ltd.

through the stimulation of potassium channels, i.e.  $K_{ATP}$  channels. This could be important in validating UDCA as an antifibrotic and antiarrhythmic drug for treatment of failing hearts and fetal arrhythmia.

© 2016 Published by Elsevier Ltd.

## 1. Introduction

Intrahepatic Cholestasis of Pregnancy (ICP) is a liver disease that affects approximately 1% pregnancies in the United Kingdom (Geenes and Williamson, 2009; Geenes et al., 2014; Glantz et al., 2004). ICP is characterised by maternal pruritus in conjunction with abnormal liver function tests and raised serum bile acids. There is also a change in bile acid pool composition, whereby the primary bile acids, taurocholic acid (TC) and taurochenodeoxycholic acid (TCDCA) predominate. ICP can be complicated by adverse events for the fetus, including spontaneous preterm labour, fetal distress, fetal arrhythmia and intrauterine death. These adverse outcomes occur more commonly in pregnancies complicated by higher maternal serum bile acid levels (Geenes and Williamson, 2009; Geenes et al., 2014; Glantz et al., 2004). The aetiology of fetal death is still poorly understood and is thought to occur suddenly (Geenes et al., 2014; Glantz et al., 2004).

Previous research in our lab focused on neonatal rat models of the fetal heart, although some work was previously carried out using isolated human fetal cardiomyocytes from aborted fetuses of 9–12 weeks of gestation with no known pathology (Gorelik et al., 2006a). These cells were used to investigate gene expression of bile acid transporters and changes in expression after TC incubation (Gorelik et al., 2006a).

The exact mechanisms through which bile acids induce arrhythmias in the human fetal heart remain unclear, although a number of studies using neonatal rat cardiomyocytes have shown that bile acids can affect heart cells. For instance, previous studies demonstrated that the bile acid TC can alter the rate and rhythm of cardiomyocyte contraction in both single cells and in a monolayer, as well as causing abnormal  $Ca^{2+}$  dynamics of single cells (Gorelik et al., 2002; Williamson et al., 2001). The main characteristics of arrhythmia induced by TC were a reduction of the contraction rate, decreased amplitude of contraction, calcium overload, irregularity of contraction within a beating cell, and desynchronization of a network of cardiomyocytes.

Cardiomyocytes are not the only cells in the heart; fibroblasts make up a large proportion of cells during development and may therefore also be affected by bile acids (Banerjee et al., 2007; Miragoli et al., 2011a). Miragoli et al. (2011a) showed that  $\alpha$ -Smooth Muscle Actin-positive ( $\alpha$ SMA) myofibroblasts transiently appear during gestation, but are not found in postnatal hearts (Miragoli et al., 2011a). This led to the development of the fetal heart model consisting of neonatal rat cardiomyocytes coated with neonatal rat myofibroblasts, which was compared to a neonatal rat cardiomyocytes only model to simulate the maternal heart (Miragoli et al., 2011a). Using these models, Miragoli et al. (2011a) showed that TC induces arrhythmias only in the fetal heart model of neonatal rat cardiomyocytes and myofibroblasts, but not in the cardiomyocytes only model (Miragoli et al., 2011a).

Ursodeoxycholic acid (UDCA) is a commonly used treatment for ICP, and is currently in clinical trials for ICP as well as adult heart disease, although the effects of UDCA on the fetus have not been fully delineated. Geenes et al. (2014) showed that in ICP pregnancies treated with UDCA, elevated concentrations of the drug (0.6–2.60  $\mu$ mol/L UDCA) were found in cord blood samples (Geenes et al., 2014).

Using the neonatal rat models, Miragoli et al. (2011a) showed that co-incubation of UDCA with TC abolishes the arrhythmic effect of TC in the neonatal rat cardiomyocytes and fibroblasts model (Miragoli et al., 2011a). Conduction velocity was shown to be increased upon treatment with UDCA in this model, but did not change in the cardiomyocytes only model (Miragoli et al., 2011a). However, the toxicity of UDCA in neonatal rat cardiomyocytes and fibroblasts has not yet been investigated.

During the organogenic period of embryonic development many developing areas undergo partial hypoxia, as indicated by the hypoxia marker pimonidazole. These hypoxic areas change depending upon the age of the fetus (Webster and Abela, 2007). Pimonidazole also co-localises with cardiac developmental markers including vascular endothelial growth factor (VEGF) and hypoxia inducible factor (HIF-1 $\alpha$ ). It can therefore be speculated that the relative state of chronic hypoxia in which the human heart develops is necessary for the normal development of the cardiovascular system (Webster and Abela, 2007). Clancy et al. (2007) showed that hypoxia is thought to contribute to differentiation of human fetal cardiac fibroblasts into myofibroblasts *in vitro* (Clancy et al., 2007). It has also been postulated that fetal death in ICP may be mediated by bile acid induced vasoconstriction of placental vessels leading to acute hypoxia in these fetuses (Mays, 2010; Sepúlveda et al., 1991). A study by Miragoli et al. (2011a) showed that myofibroblasts transiently appear in human fetal ventricular tissue during the second and third trimesters of gestation. This may have an influence on ICP-related fetal heart arrhythmia and sudden fetal death, which is thought to occur abruptly at late gestation (Miragoli et al., 2011a).

It was previously postulated that UDCA acts through ATP-dependent potassium ( $K_{ATP}$ ) channels (Miragoli et al., 2011a).  $K_{ATP}$  channels are well established pharmacological targets that control cellular energy production through alteration of electrical properties of the membrane of the cell. A recent study has demonstrated that the membrane potential of isolated fibroblasts can be regulated by  $K^+$  current (Chilton et al., 2005; Shibukawa et al., 2005).

Although several different types of  $K^+$  channels were shown to be expressed in cardiac fibroblasts, we focused specifically on  $K_{ATP}$  channel function (Chilton et al., 2005; Shibukawa et al., 2005; Walsh and Zhang, 2008). We investigated the ability of selective  $K_{ATP}$  channel openers pinacidil and P1075 (N-cyano-N'-(1,1-dimethylpropyl)-N''-3-pyridylguanidine) to modulate resting membrane potential (RMP) in cultured fibroblasts.

Pinacidil is indicated in the management of hypertension, as it induces vasorelaxation (Lange et al., 2002). Pinacidil acts on the sulphonylurea receptor subunits (SUR) of the  $K_{ATP}$  channel, which enhances the ability of SURs to bind and hydrolyse MgATP. This leads to  $K_{ATP}$  channel opening causing potassium efflux, which in turn hyperpolarizes the cell membrane (Lange et al., 2002). In a study using cardiac fibroblasts from an infarcted heart model, pinacidil treatment increased whole-cell  $K_{ATP}$  current which was blocked by glibenclamide (Benamer et al., 2013). It is thought that activation of fibroblast  $K_{ATP}$  current would reduce the depolarizing effect on cardiomyocytes, which would subsequently prevent early after depolarisations. Another agent used in the present study, P1075 is a more potent analogue of pinacidil (Lange et al., 2002).

Although  $K_{ATP}$  channel subunits are abundant in

cardiomyocytes, Benamer et al. (2009, 2013) reported mRNA and protein expression of SUR2 and Kir6.1 as the two most prominently expressed subunits in mouse and rat ventricular fibroblasts (Benamer et al., 2013, 2009). Subsequently, they recorded current carried by the Kir6.1/SUR2 channel complex, which was shown to be sensitive to both pinacidil and glibenclamide. They demonstrated a connection between  $K_{ATP}$  channel activation by pinacidil and fibroblast proliferation (Benamer et al., 2009). Interestingly,  $K_{ATP}$  subunits were detected not earlier than day 7 of fibroblast culture, and their expression increased progressively alongside  $\alpha$ SMA. This suggests that  $K_{ATP}$  subunit co-expression may be dependent on fibroblast differentiation into myofibroblasts, which in turn has potential implications in pathophysiological conditions. Currently no evidence exists from human fibroblasts on  $K_{ATP}$  channel localisation and functional contribution to membrane potential. This would be particularly relevant in relation to electrical coupling of fibroblasts and cardiomyocytes under adverse conditions such as arrhythmia.

In this study, human fetal cardiac tissues were collected and using new isolation methods we obtained human fetal cardiomyocytes and fibroblasts. Firstly, we characterised the human fetal cardiomyocytes and fibroblasts. Secondly, we compared calcium transient characteristics of human fetal cardiomyocytes with those of neonatal rat cardiomyocyte-fibroblast co-cultures and investigated the effect of TC and UDCA on these cells. Finally, as the fetus develops in a partially hypoxic environment, we investigated the effect of hypoxia on human fetal and neonatal rat fibroblasts.

## 2. Materials and methods

### 2.1. Isolation methods

Isolation of cardiomyocytes and fibroblasts from 1 to 2 day old Sprague–Dawley rats was performed in accordance with the guidelines of the UK Home Office Animal (Scientific Procedures) Act of 1986. Neonatal rat cardiac cells were isolated using a gentleMACS Dissociator (Miltenyi Biotec) according to their protocol for rodent neonatal hearts ([www.miltenyibiotec.com/protocols](http://www.miltenyibiotec.com/protocols)). After dissociation of the neonatal rat cells, fibroblasts were separated from cardiomyocytes by preplating the cells in Medium 199 (M199, Sigma) containing 10% neonatal calf serum (NCS, Biosera), 1% L-Glutamine (Sigma), 0.5% antibiotics (Sigma) and 1% Vitamin B12 (Sigma) for 1 h at 37 °C in 1% CO<sub>2</sub> in a flask, as previously described (Miragoli et al., 2011a). The supernatant containing the neonatal rat cardiomyocytes was then collected and the cardiomyocytes were seeded as a confluent monolayer (250,000 cells per 13 mm coverslip) on the day of isolation in M199 containing 10% NCS and supplements. New M199 containing 10% NCS and supplements was added to the flask. The subsequent day neonatal rat fibroblasts from the previous isolation (after 8 days) labelled with Vybrant Dil were seeded on top of the cardiomyocytes in a 1:10 FB:CM ratio in M199 containing 5% NCS. Neonatal rat cardiomyocytes were maintained in culture for up to 5 days and fibroblasts were maintained for up to 10 days.

Human fetal hearts were obtained from surgical terminations of pregnancy at 12–17 weeks of gestation, which were terminated due to scan or genetic abnormalities, after prior consent of the mother using Biobank ethical approval. Fetal human cardiomyocytes and fibroblasts were isolated using solutions from the neonatal heart kit (Miltenyi Biotec). Human fetal cardiomyocytes and fibroblasts were separated using the preplating technique described above, which was carried out for 2 h for co-cultures; 3 h for cardiomyocyte only and were subsequently seeded at approximately 100,000 cells per glass bottom dish (Mattek). All human fetal cardiac cells were maintained in M199 with 10% NCS and

supplements as above. Human fetal cardiomyocytes were maintained in culture for up to 10 days, fibroblasts were cultivated for up to a month.

All cardiomyocytes and fibroblasts were cultured on 13 mm glass coverslips or glass bottom dishes (Mattek) coated with laminin (0.5  $\mu$ g/mL) at 37 °C in 1% CO<sub>2</sub>. 24 h treatment of fibroblasts with hypoxia was carried out at 37 °C, 1% CO<sub>2</sub> and 8% O<sub>2</sub>. Fibroblasts were maintained in M199 with 10% NCS and supplements. Cardiomyocytes and fibroblasts were treated with 10 nM - 1  $\mu$ M UDCA (Sigma), 0.1–0.5 mM TC (Sigma), 20  $\mu$ M glibenclamide (Sigma), 10–30  $\mu$ M P1075 (Tocris) or 100  $\mu$ M pinacidil (Sigma), alone or in combination, acutely (for up to an hour) or as pre-treatment (chronic) for 24 h in normoxia or hypoxia. The range of UDCA and TC was used for experiments investigating the potentially negative effects of these drugs on the cells. The choice of 1  $\mu$ M UDCA was taken from [<sup>3</sup>H]-Glibenclamide experiments with neonatal rat fibroblasts, whereby there is displacement of the [<sup>3</sup>H]-Glibenclamide by UDCA (Miragoli et al., 2011a). Although a higher concentration of TC was used compared to the levels found in mother and fetus, this concentration was chosen to potentially mimic the longer lasting effects of the bile acids on the fetus, which cannot be replicated in a cell culture model. In addition, the concentrations were significantly reduced compared to previously published work (Gorelik et al., 2002; Miragoli et al., 2011a; Sheikh Abdul Kadir et al., 2010; Williamson et al., 2001).

### 2.2. Electrophysiological recordings

Membrane potential was measured using sharp electrode impalement of single fibroblasts. Impalement was carried out on a Nikon Eclipse TE300 using an Axopatch -1D (Axon Instruments) with Clampex 8.0 to record resting membrane potential (RMP). Neonatal rat and human fetal fibroblasts were maintained on the system with HBSS containing 1% NCS. Cells were impaled by sharp nanopipettes containing 3 M KCl and, after 1 min of membrane potential stabilization, 10s recordings were taken. RMP was averaged for each trace. Drug treatments were carried out acutely or after 24 h treatment, while 24 h hypoxia preceded RMP recordings. After acute (up to 1 h) treatment with TC, UDCA, glibenclamide, P1075 and pinacidil, cells were allowed to adapt for 10 min before RMP recordings.

### 2.3. Immunofluorescence

All fibroblasts and cardiomyocytes were cultured on coverslips. Fibroblasts were allowed to proliferate until optimal density before 24 h treatment with normoxia/hypoxia and/or UDCA. Subsequently the preparations were washed with PBS and fixed in 4% PFA (Sigma) for 10 min. Coverslips were incubated in blocking buffer (PBS, 20% serum, 5% BSA, 0.05% Tween-20), after which primary antibodies diluted in blocking buffer were applied:  $\alpha$ -Smooth Muscle Actin ( $\alpha$ SMA, Abcam for rat, DAKO for human work),  $\alpha$ -Actinin, Connexin43 (Sigma) and Vimentin (Thermo Scientific). After washes with PBS, coverslips were incubated with secondary antibodies, AlexaFluor488 or AlexaFluor546 (Invitrogen) and DAPI (Molekula), before being washed and mounted. Calculations of the % $\alpha$ SMA positive cells were carried out using an epifluorescence microscope (Nikon) using 40 $\times$  (oil) magnification. If  $\alpha$ SMA structures were visible in the cell, it was deemed positive.

### 2.4. Scanning ion conductance microscopy

Scanning Ion Conductance Microscopy (SICM) was used to image cell morphology and topography. SICM is a non-contact method of imaging the topography of intact cells (Miragoli et al., 2011b;

Nikolaev et al., 2010). This can be achieved by scanning the surface of the cell using a nanopipette filled with electrolyte and an electrode connected to a feedback mechanism that also receives information from a ground electrode placed in the bath. Using the ion current as a feedback mechanism the distance between the pipette tip and sample can be maintained, since there is a drop in current when the pipette approaches the cell surface. This enables high resolution scans of cell surface areas of varying size to be generated.

### 2.5. Optical recording of calcium transients and action potentials

Co-cultures were allowed to mature until beating cardiomyocytes could be seen. For neonatal rat cultures this required 3–5 days and 3–8 days for human fetal cultures. Cells were incubated in 1 mL of medium containing either 5  $\mu$ M Fluo4 acetoxymethyl ester (Fluo4 AM, Invitrogen) for 20 min or 1  $\mu$ M Di-8-ANEPPS (4-(2-[6-(Diocetylamin)-2-naphthalenyl] ethenyl)-1-(3-sulfopropyl) pyridinium inner salt; Biotium Bioscience, Germany), for 5 min at 37 °C. HBSS was used for experiments, which was prepared by addition of Phenol Red Free Hanks Balanced Salts (Sigma), 0.35 g/L Sodium Bicarbonate (Sigma) and 2.38 g/L HEPES (VWR) to 1 L dH<sub>2</sub>O. After incubation the coverslip was washed in HBSS and mounted on an inverted microscope (Nikon Eclipse TI) with a camera for optical recording (MICAM Ultima) and perfused at 35 °C. Different filters were used for imaging with Fluo4 AM, Di-8-ANEPPS and to visualise Vybrant Dil stained Fibroblasts. Neonatal rat cultures were paced at a frequency of 1 Hz. Pacing was also applied to human fetal cultures, although cells showed a spontaneous loss of activity, particularly after TC treatment and did not follow pacing consistently. Cells were allowed to adapt for 10 min before control videos were taken using the imaging software (Scimedia, Japan). Subsequently, treatment with TC and/or UDCA was carried out for 10 min before additional recordings were obtained. The duration of the videos taken for treatment with 0.1 mM TC and TC in combination with UDCA was 4 – 8s with a frame rate of 1–2 frames/ms. Recordings were averaged based on the whole area recorded, containing cardiomyocytes only or both co-cultured cardiomyocytes and fibroblasts. Analysis of the data was carried out using BV\_Analyse v11.08 (Brainvision, Scimedia) or Matlab.

### 2.6. Experiments of spontaneous beating activity

Spontaneous beating rate was assessed in clusters of beating neonatal rat cardiomyocytes at 35 °C, which were allowed to adapt to HBSS for 10 min. Activity was measured from 10 different regions, for control, TC and TC in combination with UDCA. An inter-drug interval of 10 min was allowed for adaptation to the treatments.

### 2.7. Data analysis

Statistical analysis for all data was carried out using Graphpad Prism 5. Data are shown as mean with standard error of the mean (SEM), unless otherwise stated. The number of isolations of neonatal cells (of litters of approximately 12 pups) or tissue samples in case of human tissue is indicated by 'i' as described in the figure legend and text. The number of recordings (optical recording), cells (impalement) or images is designated with 'n'. For optical recording the n and i are given for the first parameter, subsequent parameters of the same cell type were analysed using the same data sets. All data were tested for normality using the Kolmogorov–Smirnov test and evaluated for Gaussian distribution using parametric tests. Otherwise, non-parametric equivalents were used. A p-value of  $p \leq 0.05$  (\*),  $p \leq 0.01$  (\*\*), or  $p \leq 0.001$  (\*\*\*) was deemed significant. For the analysis of more than two

categories, an One-way Analysis of Variance (One-way ANOVA) with post-hoc Bonferroni correction, or non-parametric equivalent, a Kruskal–Wallis ANOVA with Dunns correction was used.

## 3. Results

### 3.1. Characterisation of human fetal cardiomyocytes

For the first time we established cultures of beating cardiomyocytes from human fetal tissues. We characterised human fetal cardiomyocytes by immunofluorescence staining using a number of cardiac markers including  $\alpha$ -Actinin and Connexin43. We found that the cells expressed  $\alpha$ -Actinin [Fig. 1A–B], similar to neonatal rat cardiomyocytes [Fig. 1C]. Cell topography was compared to the neonatal cardiomyocytes and fibroblasts using SICM [Fig. 1D–E]. To allow the identification of the different cell types for SICM experiments, neonatal rat fibroblasts were labelled with a fluorescent marker (Vybrant Dil) before seeding [Fig. 1E]. There are differences in topography and cell size between human fetal [Fig. 1A, D] and human adult cardiomyocytes (Lyon et al., 2009). Adult cardiomyocytes show clear striated patterns of  $\alpha$ -Actinin associated with the well organised T-tubular structures (Gorelik et al., 2013; Lyon et al., 2009; Nikolaev et al., 2010). Although both human fetal and neonatal rat cardiomyocytes show striated patterns, their surface topography shows no T-tubular invaginations or Z-grooves, as seen in human (or rodent) adult cardiomyocytes, indicating that cells are still undergoing structural development (Gorelik et al., 2013; Lyon et al., 2009; Nikolaev et al., 2010). The human fetal cardiac cells were larger than the neonatal rat cardiac cells, although neither showed the invaginations or grooves associated with adult cardiomyocytes (Gorelik et al., 2013; Lyon et al., 2009; Nikolaev et al., 2010). Connexin43 expression indicates that human fetal cardiomyocytes can form gap junctions in culture [Fig. 1A]. A natural infiltration of Vimentin-positive fibroblasts occurred in human fetal cultures after 2 h preplating [Fig. 1B]. Immunostaining for  $\alpha$ SMA revealed the presence of  $\alpha$ SMA-positive neonatal rat myofibroblasts interspersed in the  $\alpha$ -Actinin-positive neonatal rat cardiomyocytes culture [Fig. 1C].

### 3.2. UDCA does not affect calcium handling properties of neonatal rat cardiomyocytes

Analysis of calcium transient duration, as measured by 90% recovery to baseline, can provide information on changes in excitation-contraction coupling and calcium handling in the cells. There was no significant difference in calcium transient duration (90%) of neonatal rat cardiomyocytes under control conditions (333.0 ms  $\pm$  8.4; n = 66, i = 6,  $p > 0.05$ ) and in the presence of increasing concentrations of UDCA: 10 nM (389.3 ms  $\pm$  22.6; n = 7, i = 2), 100 nM (338.2 ms  $\pm$  12.7; n = 28, i = 2) and 1  $\mu$ M (345.0 ms  $\pm$  19.0; n = 10, i = 2) [Fig. 2A]. This indicated that UDCA did not affect calcium transient parameters in cardiomyocytes at concentrations similar to those found to cross the placenta in ICP pregnancies treated with UDCA (Geenes et al., 2014).

Similarly, no significant difference was found in calcium transient duration (90%) of neonatal rat cardiomyocytes cultured with fibroblasts under control conditions (382.7 ms  $\pm$  7.3; n = 77, i = 6,  $p > 0.05$ ) and in the presence of increasing concentrations of UDCA: 10 nM (394.3 ms  $\pm$  5.4; n = 71, i = 2), 100 nM (337.4 ms  $\pm$  11.0; n = 35, i = 2), 1  $\mu$ M (407.6 ms  $\pm$  4.0; n = 38, i = 2) and 100  $\mu$ M UDCA (444.1 ms  $\pm$  3.1; n = 6, i = 2) [Fig. 2B].

In addition, time to peak was affected neither in the cardiomyocytes only cultures after treatment with 10 nM (80.1 ms  $\pm$  7.0), 100 nM (89.9 ms  $\pm$  7.5) or 1  $\mu$ M UDCA (78.0 ms  $\pm$  6.6) compared to control (79.4 ms  $\pm$  2.9;  $p > 0.05$ )

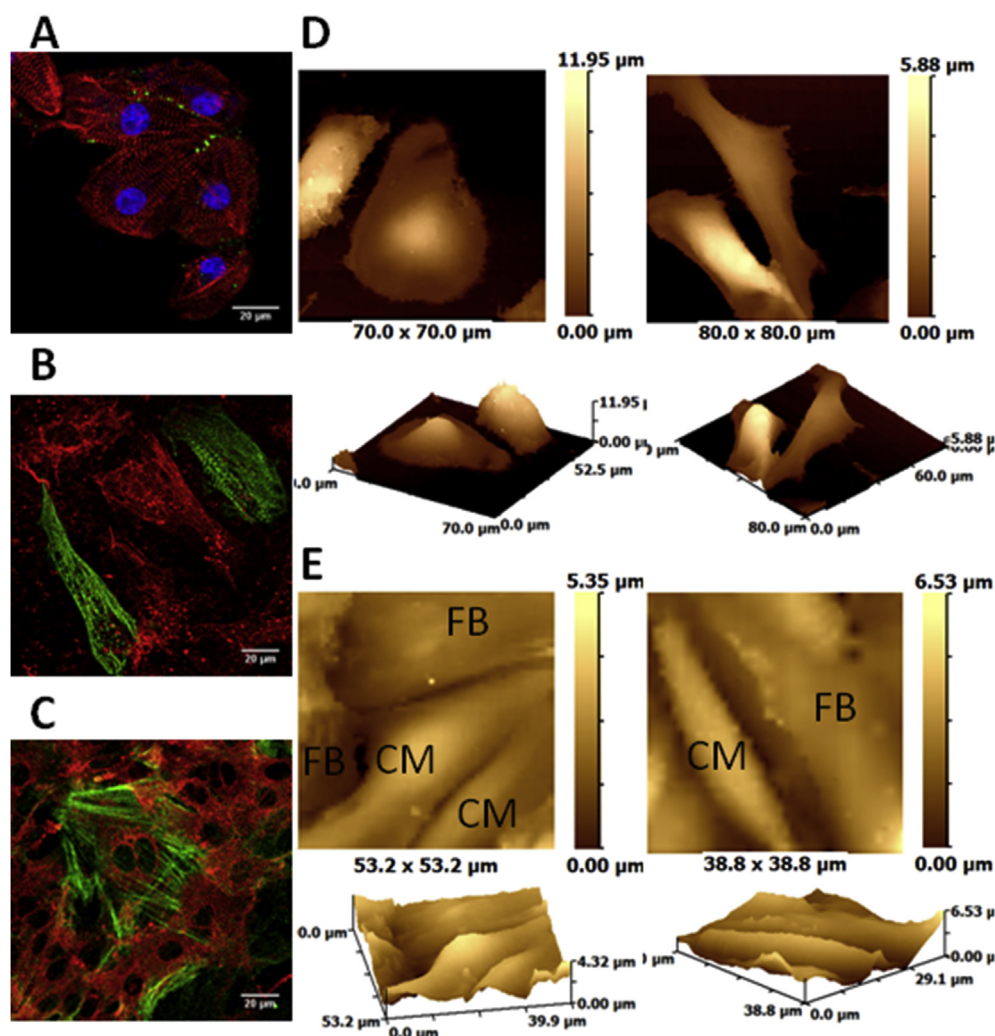


**Fig. 1. Characterisation of the human fetal cardiac cells.** Human fetal cardiomyocytes and fibroblasts were isolated and characterised using immunofluorescence microscopy and SICM. A)  $\alpha$ -Actinin (red) and Connexin43 (green) staining of the human fetal cardiomyocytes show gap junction formation between the  $\alpha$ -Actinin positive cardiomyocytes. Scale bar: 20  $\mu$ M. B)  $\alpha$ -Actinin (green) and Vimentin (red) stained cardiomyocyte cultures show infiltration of Vimentin positive fibroblasts. Scale bar: 20  $\mu$ M. C) Co-cultures of neonatal rat cardiac cells, similar to the human fetal culture, was achieved by culturing  $\alpha$ -Actinin-positive cardiomyocytes (red) and  $\alpha$ -Smooth Muscle Actin-positive myofibroblasts (green) together. D) SICM topography scans show variability in the size and shape of the human fetal cardiomyocytes and fibroblasts. E) Neonatal rat cardiomyocytes and fibroblasts form a dense monolayer of cells when cultured together. Cardiomyocytes and fibroblasts are distinguishable by the Dil labelling (not visible here).

[Fig. 2C], nor in the co-cultures after treatment with 10 nM ( $47.5 \text{ ms} \pm 1.2$ ), 100 nM ( $48.7 \text{ ms} \pm 2.0$ ) or 1  $\mu$ M UDCA ( $48.0 \text{ ms} \pm 1.8$ ) compared to control ( $48.2 \text{ ms} \pm 2.1$ ;  $p > 0.05$ ) [Fig. 2D].

Finally, no significant difference was measured in the total calcium amplitude ( $\Delta F/F_0$ ) in the co-cultures after treatment with 10 nM ( $57.2 \text{ a.u.} \pm 1.7$ ), 100 nM ( $43.4 \text{ a.u.} \pm 1.6$ ) or 1  $\mu$ M UDCA ( $53.9 \text{ a.u.} \pm 1.9$ ) compared to control ( $53.2 \text{ a.u.} \pm 2.6$ ;  $p > 0.05$ ) [Fig. 2E].

### 3.3. Taurocholic acid induces changes in calcium transient duration which are attenuated by UDCA

Miragoli et al. (2011a) previously showed that UDCA attenuated TC-induced conduction velocity slowing and prevented TC-induced re-entries in the co-culture model of neonatal rat cardiomyocytes and fibroblasts (Miragoli et al., 2011a). To expand upon this work, the effects of TC alone and in combination with UDCA were investigated in this model using optical recording of calcium transients.

Unlike UDCA, the addition of 0.1 mM TC ( $608.8 \text{ ms} \pm 23.3$ ;  $n = 8$ ,  $i = 4$ ,  $p \leq 0.001$ ) significantly prolonged calcium transient duration in neonatal rat cardiomyocytes cultured with fibroblasts in comparison to control ( $382.0 \text{ ms} \pm 72.2$ ;  $n = 18$ ,  $i = 4$ ), whilst treatment with 0.1 mM TC in combination with 1  $\mu$ M UDCA resulted in a similar calcium transient duration to that of control ( $326.3 \text{ ms} \pm 95.3$ ;  $n = 8$ ,  $i = 2$ ) [Fig. 3A]. A significant reduction in transient duration was seen after combined treatment with TC and UDCA ( $326.3 \text{ ms} \pm 95.3$ ;  $p \leq 0.05$ ) compared to TC alone ( $608.8 \text{ ms} \pm 23.3$ ).

There was a significant increase in time to peak after TC treatment ( $69.73 \text{ ms} \pm 4.1$ ;  $p \leq 0.001$ ) compared to control ( $50.08 \text{ ms} \pm 1.6$ ). This was attenuated by UDCA in the combined treatment ( $54.38 \text{ ms} \pm 4.0$ ;  $p \leq 0.05$ ) [Fig. 3B].

In human fetal cardiomyocyte cultures an increased presence of fibroblasts was observed due to increased culture time. Therefore no additional fibroblasts were added as in the neonatal rat model [Fig. 3C, D left]. To reduce the amount of fibroblast infiltration additional experiments were carried out after 3 h of preplating for 1

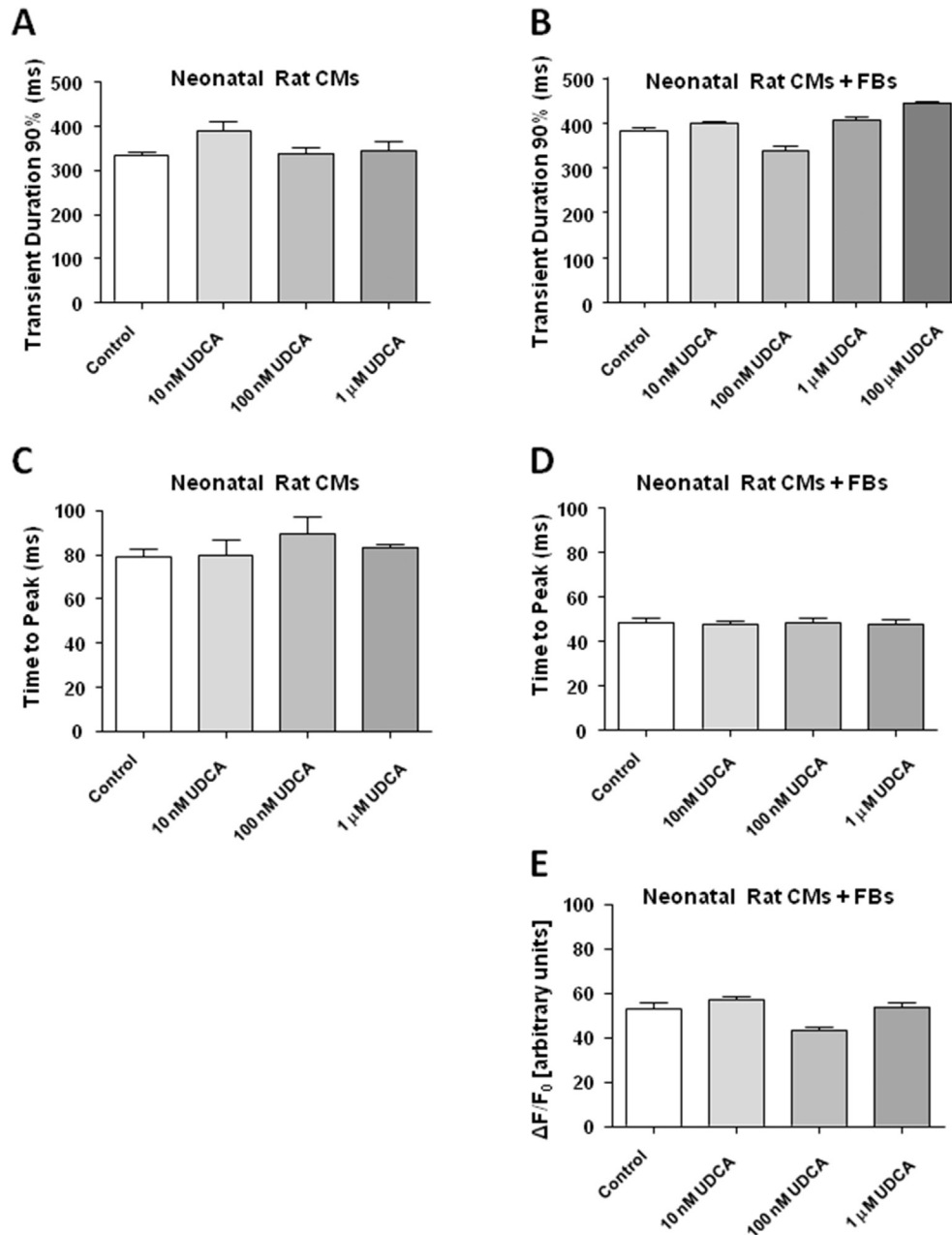


**Fig. 2. UDCA does not affect calcium transients of neonatal rat cardiomyocytes.** The effect of UDCA on the calcium transient dynamics of neonatal rat cardiomyocytes cultured alone or in combination with fibroblasts was investigated. A) There was no significant change in calcium transient duration, as measured by 90% recovery, when neonatal cardiomyocytes were acutely treated with increasing doses of UDCA; 10 nM ( $n = 7$  recordings,  $i = 2$  isolations), 100 nM ( $n = 28$ ,  $i = 2$ ) and 1  $\mu$ M ( $n = 10$ ,  $i = 2$ ) compared to control ( $n = 66$ ,  $i = 6$ ,  $p > 0.05$ ). B) Similarly, there was no significant difference in the calcium transient duration of neonatal rat cardiomyocytes when cultured together with fibroblasts after treatment with UDCA; 10 nM ( $n = 71$ ,  $i = 2$ ), 100 nM ( $n = 35$ ,  $i = 2$ ), 1  $\mu$ M ( $n = 38$ ,  $i = 2$ ) and 100  $\mu$ M UDCA ( $n = 6$ ,  $i = 2$ ) compared to control ( $n = 77$ ,  $i = 6$ ). C) No significant change was found in the time to peak when treating neonatal cardiomyocytes with increasing doses of UDCA (10 nM, 100 nM or 1  $\mu$ M) compared to control. D) No significant change was found in the time to peak when treating neonatal cardiomyocytes co-cultured with fibroblasts with increasing doses of UDCA (10 nM, 100 nM or 1  $\mu$ M) compared to control. E) Treatment with increasing doses of UDCA (10 nM, 100 nM or 1  $\mu$ M) did not lead to significant changes in  $\text{Ca}^{2+}$  amplitude in the neonatal rat cardiomyocyte and fibroblast co-culture.

isolation [Fig. 3C, D right].

There was a significant increase in calcium transient duration after incubation with 0.1 mM TC ( $180.7 \text{ ms} \pm 26.0$ ;  $n = 15$ ,  $i = 2$ ,  $p \leq 0.05$ ) compared to control ( $144.4 \text{ ms} \pm 15.2$ ;  $n = 51$ ,  $i = 3$ ) [Fig. 3C]. Addition of 1  $\mu$ M UDCA and 0.1 mM TC showed that UDCA attenuated the increase in calcium transient duration induced by TC ( $119.4 \text{ ms} \pm 11.1$ ;  $n = 55$ ,  $i = 2$ ,  $p \leq 0.001$ ) [Fig. 3C]. Additionally, after 3 h of preplating, preliminary data indicates that no changes in calcium transient duration occurred after incubation with 0.1 mM TC ( $149.4 \text{ ms} \pm 6.3$ ;  $n = 4$ ,  $i = 2$  dishes, 1 isolation)

compared to control ( $193.6 \text{ ms} \pm 9.8$ ;  $n = 5$ ,  $i = 2$  dishes, 1 isolation).

Incubation with TC also led to a significant increase in time to transient peak ( $65.2 \text{ ms} \pm 3.4$ ;  $p \leq 0.001$ ) compared to control ( $37.7 \text{ ms} \pm 4.3$ ) [Fig. 3D]. This increase was prevented when UDCA was applied together with TC ( $38.0 \text{ ms} \pm 4.5$ ). Additionally, after 3 h of preplating, preliminary data indicates that no changes in time to peak occurred after incubation with TC ( $53.3 \text{ ms} \pm 2.1$ ) compared to control ( $58.6 \text{ ms} \pm 4.0$ ).

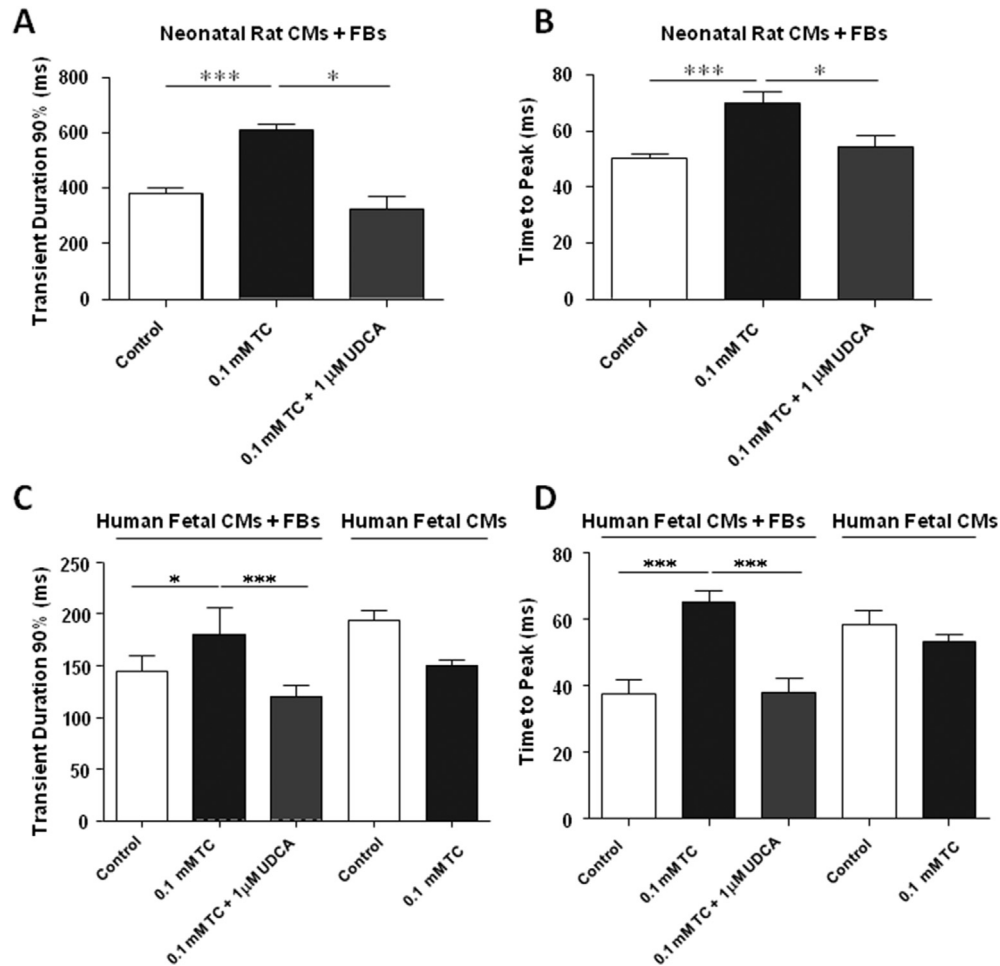


**Fig. 3. TC induces calcium transient duration prolongation which is reversed by UDCA.** A) Optical recording of neonatal rat cardiomyocytes and fibroblasts shows that 0.1 mM TC ( $n = 8$  recordings,  $i = 4$  isolations,  $p \leq 0.001$ ) leads to calcium transient duration prolongation compared to control ( $n = 18$ ,  $i = 4$ ), whilst this was prevented when the cells were treated with TC in combination with 1 μM UDCA ( $n = 8$ ,  $i = 2$ ,  $p \leq 0.05$ ). B) Time until full release was also prolonged after 0.1 mM TC incubation ( $p \leq 0.001$ , compared to control) and this was prevented by 1 μM UDCA ( $p \leq 0.05$ , compared to TC). Similarly in a culture of human fetal cardiomyocytes, which showed a higher level fibroblast infiltration, TC induced increases in calcium transient duration and time to peak ( $n = 15$ ,  $i = 2$ ,  $p \leq 0.05$  and  $p \leq 0.001$  respectively) compared to control ( $n = 51$ ,  $i = 3$ ), was reversed by 1 μM UDCA ( $n = 55$ ,  $i = 2$ ,  $p \leq 0.001$ ) (C, D left). In human fetal cultures with little fibroblast infiltration, 0.1 mM TC ( $n = 4$ ,  $i = 2$  dishes, 1 isolation) did not induce a significant increase in either calcium transient duration or in time to peak ( $n = 5$ ,  $i = 2$  dishes, 1 isolation) (C, D right).

#### 3.4. Action potential duration and beating rate are altered by TC

Changes in calcium transient duration may be due to changes in action potential duration and repolarisation time. We investigated the effect of TC on action potential duration (APD) in the co-culture model of neonatal rat cardiomyocytes and fibroblasts [Fig. 4A]. Addition of 0.2 mM TC ( $271.0 \text{ ms} \pm 41.0$ ;  $n = 20$ ,  $i = 3$ ,  $p \leq 0.001$ ) led to a significant increase in action potential duration at 90% repolarization (APD90%) in comparison to control ( $242.1 \text{ ms} \pm 26.5$ ;  $n = 21$ ,  $i = 3$ ). When 1 μM UDCA ( $226.5 \text{ ms} \pm 29.0$ ;  $n = 12$ ,  $i = 3$ ,  $p \leq 0.001$ ) was subsequently added to 0.2 mM TC, a significant reduction in APD90% was observed in comparison to TC alone.

Changes in calcium dynamics and action potential characteristics led to changes in contraction rate and rhythmicity of the cells. The spontaneous beating rate of neonatal rat cardiomyocytes in co-culture with fibroblasts showed changes with TC alone and TC combined with UDCA treatment [Fig. 4B]. The baseline control was set as 100% ( $n = 86$ ,  $i = 4$ ), deviation from the baseline was calculated for 0.1 mM TC and for 0.1 mM TC together with 1 μM UDCA [Fig. 4B]. Incubation with 0.1 mM TC led to a significant reduction in beating rate compared to baseline ( $71.3\% \pm 3.0$ ;  $n = 80$ ,  $i = 4$ ,  $p \leq 0.001$ ). Co-incubation of 0.1 mM TC and 1 μM UDCA led to

a partial, but significant improvement in beating rate when compared to TC ( $87.6\% \pm 2.6$ ;  $n = 27$ ,  $i = 4$ ,  $p \leq 0.001$ ).

#### 3.5. Bile acids modulate resting membrane potential in fibroblasts but not in cardiomyocytes

The effect of bile acids on fibroblast resting membrane potential (RMP) was investigated to evaluate whether changes in calcium transients of cardiomyocytes were due to changes in resting membrane potential of fibroblasts [Fig. 5A (rat) and 5C (human)] and/or cardiomyocytes [Fig. 5B]. 0.2 mM TC and 0.2 mM TC combined with 100 nM UDCA did not affect the RMP of neonatal rat cardiomyocytes (0.2 mM TC;  $-66.0 \text{ mV} \pm 6.6$ ;  $n = 3$ ;  $i = 2$ , 0.2 mM TC and 100 nM UDCA;  $-82.2 \text{ mV} \pm 1.0$ ;  $n = 4$ ,  $i = 2$ , 100 nM UDCA;  $-78.2 \text{ mV} \pm 2.1$ ;  $n = 12$ ,  $i = 2$ ) compared to control ( $-66.2 \text{ mV} \pm 3.9$ ;  $n = 20$ ,  $i = 2$ ) [Fig. 5B]. However, the RMP of both neonatal rat fibroblasts (control;  $-18.1 \text{ mV} \pm 2.5$ ;  $n = 30$ ,  $i = 3$ ) [Fig. 5A] and human fetal fibroblasts ( $-21.7 \text{ mV} \pm 1.0$ ;  $n = 78$ ,  $i = 4$ ) [Fig. 5C] became more negative following the application of 1 μM UDCA ( $-34.8 \text{ mV} \pm 3.9$ ;  $n = 28$ ,  $i = 3$ ,  $p \leq 0.01$ ;  $-41.0 \text{ mV} \pm 2.1$ ;  $n = 85$ ,  $i = 4$ ,  $p \leq 0.001$ , respectively), after 0.2 mM TC treatment the RMP became more positive in both neonatal rat and human fetal

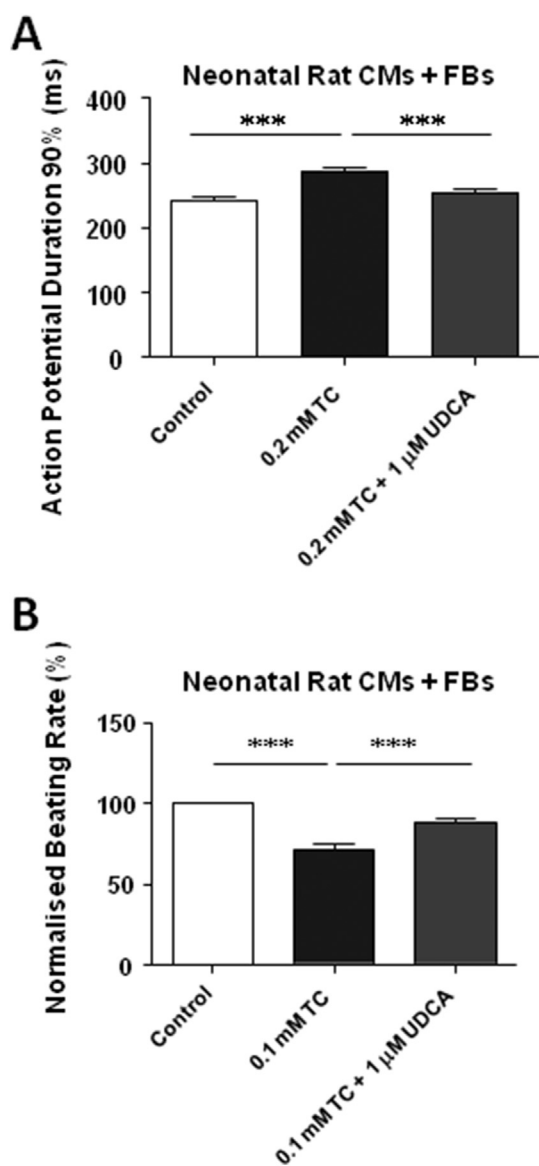


**Fig. 4. TC alters action potential parameters and beating rate, which is prevented by UDCA.** A) 0.2 mM TC ( $n = 20$  recordings,  $i = 3$  isolations) induced a significant increase in action potential duration compared to control ( $n = 21$ ,  $i = 3$ ,  $p \leq 0.001$ ), whilst this was reversed by 1  $\mu$ M UDCA ( $n = 12$ ,  $i = 3$ ,  $p \leq 0.001$ ). B) Contraction of the cardiomyocytes is usually rhythmic and regular, but treatment with 0.1 mM TC ( $n = 80$ ,  $i = 4$ ,  $p \leq 0.001$ ) induced a reduction in beating rate of the cardiomyocytes in the co-culture compared to control ( $n = 86$ ,  $i = 4$ ). Co-incubation of 0.1 mM TC and 1  $\mu$ M UDCA led to a partial, but significant improvement in beating rate when compared to TC ( $n = 27$ ,  $i = 4$ ,  $p \leq 0.001$ ).

fibroblasts ( $-6.6 \text{ mV} \pm 0.7$ ;  $n = 35$ ,  $i = 3$ ,  $p \leq 0.001$ ;  $-17.9 \text{ mV} \pm 0.5$ ;  $n = 47$ ,  $i = 3$ ,  $p \leq 0.05$ , respectively). The RMP of both neonatal rat and human fetal fibroblasts were significantly more negative after TC and UDCA treatment compared to TC alone ( $-25.0 \text{ mV} \pm 2.9$ ;  $n = 7$ ,  $i = 2$ ,  $p \leq 0.001$ ;  $-26.3 \text{ mV} \pm 0.9$ ;  $n = 31$ ,  $i = 3$ ,  $p \leq 0.01$  respectively). In addition, the RMP of human fetal fibroblasts was further hyperpolarized by UDCA in the combined treatment in comparison to control ( $p \leq 0.01$ ). Both 100  $\mu$ M pinacidil ( $-43.0 \text{ mV} \pm 4.4$ ;  $n = 8$ ,  $i = 2$ ,  $p \leq 0.001$ ) and P1075 ( $-49.2 \text{ mV} \pm 1.6$ ;  $n = 7$ ,  $i = 2$ ,  $p \leq 0.001$ ) induced a significant

hyperpolarisation of the neonatal rat fibroblasts. In human fetal fibroblasts pinacidil was more potent ( $-51.5 \text{ mV} \pm 3.3$ ;  $n = 37$ ,  $i = 3$ ) when compared to P1075 ( $-32.1 \text{ mV} \pm 2.0$ ;  $n = 36$ ,  $i = 3$ ,  $p \leq 0.05$ ), both of which induced significant hyperpolarisation compared to untreated fibroblasts (P1075:  $p \leq 0.01$ ; pinacidil:  $p \leq 0.001$ ).

Blockade of  $K_{ATP}$  channels by 20  $\mu$ M glibenclamide did not induce significant changes in RMP of human fetal fibroblasts ( $-36.3 \text{ mV} \pm 3.1$ ;  $n = 14$ ,  $i = 1$ ) compared to matched controls ( $-43.9 \text{ mV} \pm 3.2$ ;  $n = 14$ ,  $i = 1$ ) [Fig. 5D]. Furthermore, addition of 20  $\mu$ M glibenclamide prevented UDCA-induced hyperpolarisation in human fetal fibroblasts ( $-48.2 \text{ mV} \pm 4.7$ ;  $n = 21$ ,  $i = 1$ ). The RMP of human fetal fibroblasts from this isolation was on average more negative than from previous isolations, potentially due to differences in genetic background or gestation. Additional recordings with 1  $\mu$ M UDCA showed that UDCA induced further hyperpolarisation also in these fibroblasts ( $-66.8 \text{ mV} \pm 4.7$ ;  $n = 23$  cells,  $i = 1$ ,  $p \leq 0.01$ ).

These results suggest that both neonatal rat and human fetal fibroblasts express functional  $K_{ATP}$  channels. Expression of the  $K_{ATP}$  channel subunits  $K_{ir}6.1$ ,  $K_{ir}6.2$ , SUR1 and SUR2 was investigated in neonatal rat cardiomyocytes and fibroblasts ( $n = 5$ ) and was normalised to the housekeeping gene GAPDH [Supplementary Fig. 1].  $K_{ir}6.1$  was found in both neonatal rat cardiomyocytes and fibroblasts.  $K_{ir}6.2$  mRNA expression levels were very low in both neonatal rat cardiomyocytes and fibroblasts. SUR1 and SUR2 were both expressed in neonatal rat cardiomyocytes and fibroblasts.

### 3.6. Chronic UDCA treatment hyperpolarises fibroblasts without affecting cardiomyocytes

The cardiac models currently in use to investigate ICP consist of cultured cells that are acutely treated with bile acids. However, in ICP the fetus can be exposed to high levels of bile acids for many weeks, depending on the gestational week at the onset of the disease. This may lead to accumulation of bile acids in the fetus, or to a chronic exposure of the fetal heart to different bile acids during development. To elucidate the chronic effect of UDCA on neonatal rat cardiomyocytes and fibroblasts, these cells were incubated with UDCA for 24 h before RMP measurements. Chronic treatment with 100 nM ( $-72.5 \text{ mV} \pm 1.9$ ;  $n = 5$ ,  $i = 2$ ), 1  $\mu$ M ( $-74.8 \text{ mV} \pm 4.6$ ;  $n = 4$ ,  $i = 2$ ) and 10  $\mu$ M ( $-74.4 \text{ mV} \pm 1.2$ ;  $n = 6$ ,  $i = 2$ ) UDCA had no significant effect on neonatal rat cardiomyocytes when compared to control ( $-75.8 \text{ mV} \pm 1.7$ ;  $n = 36$ ;  $i = 2$ ) [Fig. 6A]. In contrast, chronic treatment of neonatal rat fibroblasts with 100 nM ( $-47.3 \text{ mV} \pm 1.5$ ;  $n = 8$ ,  $i = 2$ ), 1  $\mu$ M ( $-45.5 \text{ mV} \pm 3.7$ ;  $n = 4$ ,  $i = 2$ ), 10  $\mu$ M ( $-41.6 \text{ mV} \pm 4.3$ ;  $n = 4$ ,  $i = 2$ ) and 100  $\mu$ M ( $-41.6 \text{ mV} \pm 2.9$ ;  $n = 4$ ,  $i = 2$ ) UDCA led to significant hyperpolarisation of the fibroblasts compared to untreated controls ( $-23.5 \text{ mV} \pm 1.8$ ;  $n = 40$ ,  $i = 2$ ,  $p \leq 0.001$ ) [Fig. 6B]. Chronic treatment with 100 nM UDCA also induced significant hyperpolarisation in co-cultures of neonatal rat cardiomyocytes and fibroblasts ( $-64.7 \text{ mV} \pm 3.0$ ;  $n = 9$ ,  $i = 3$ ,  $p \leq 0.01$ ) compared to control, as measured from cardiomyocytes with linked fibroblasts ( $-50.6 \text{ mV} \pm 1.5$ ;  $n = 28$ ,  $i = 3$ ) [Supplementary Fig. 2]; whilst chronic treatment with 0.1 mM–0.5 mM TC (0.1 mM:  $-41.5 \text{ mV} \pm 0.4$ ;  $n = 12$ , 0.3 mM:  $-31.3 \text{ mV} \pm 2.0$ ;  $n = 9$  and 0.5 mM:  $-32.6 \text{ mV} \pm 1.0$ ,  $n = 19$ ;  $i = 3$ ,  $p \leq 0.01$ ) induced significant depolarisation in the co-cultures compared to control.

### 3.7. The effect of hypoxia on fibroblasts is attenuated by UDCA

A fetus develops in a state of partial hypoxia during pregnancy (Clancy et al., 2007; Patterson and Zhang, 2010; Webster and Abela, 2007). Therefore, further investigation into the effect of hypoxia on neonatal rat and human fetal fibroblasts was carried out. The ratio



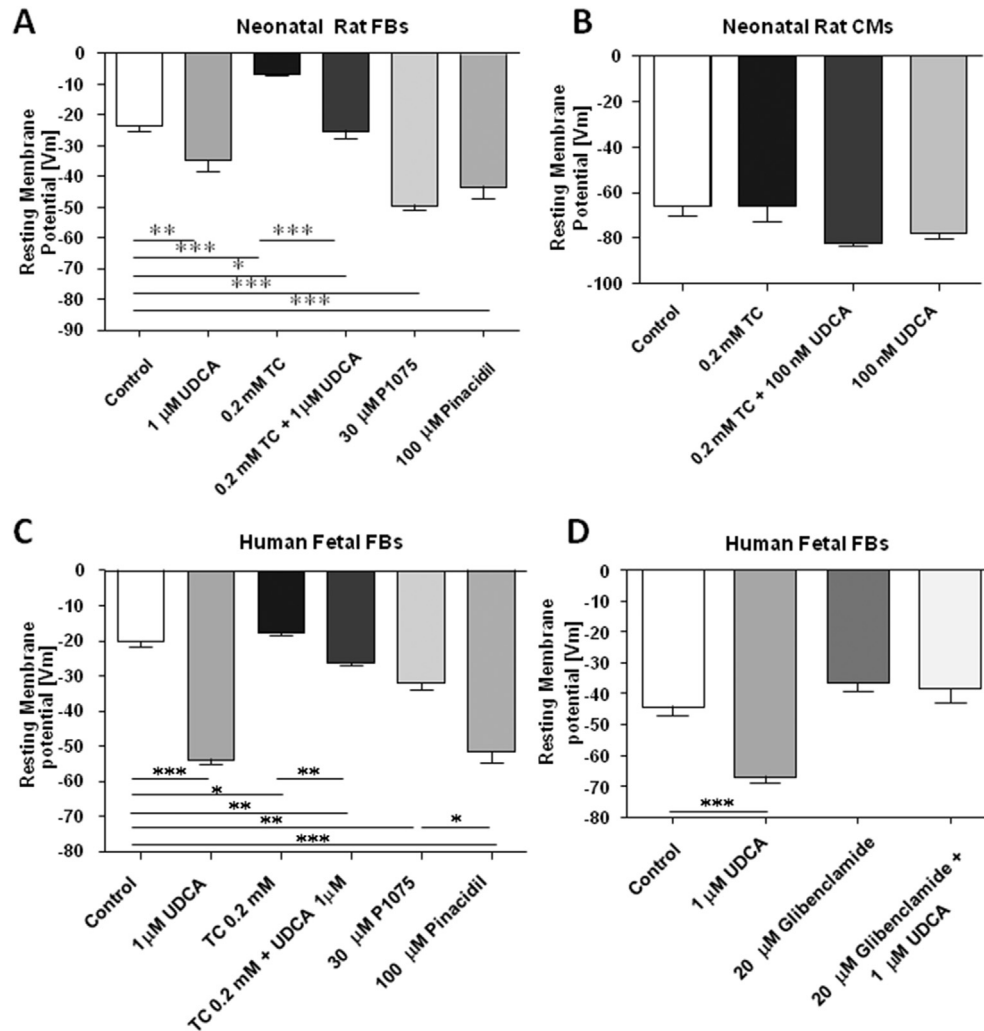


**Fig. 5. Acute effects of bile acids and  $K_{ATP}$  channel agonists on resting membrane potential in cardiomyocytes and fibroblasts.** A) Acutely applied 1  $\mu$ M UDCA ( $n = 28$  cells,  $i = 3$  isolations,  $p \leq 0.01$ ) resulted in a significant hyperpolarising shift in resting membrane potential of neonatal rat fibroblasts whilst acutely applied 0.2 mM TC ( $n = 35$ ,  $i = 2$ ,  $p \leq 0.001$ ) resulted in a significant depolarising shift in neonatal rat fibroblasts compared to control ( $n = 30$ ,  $i = 3$ ). B) Mean resting membrane potentials in neonatal rat cardiomyocytes, on the other hand remained unchanged following treatment with 0.2 mM TC ( $n = 3$ ;  $i = 2$ ), 100 nM UDCA ( $n = 12$ ,  $i = 2$ ) or 0.2 mM TC and 100 nM UDCA ( $n = 4$ ,  $i = 2$ ) compared to control ( $n = 20$ ,  $i = 2$ ). C) In human fetal fibroblasts 1  $\mu$ M UDCA treatment ( $n = 85$ ,  $i = 4$ ,  $p \leq 0.001$ ) also led to a significantly hyperpolarising shift compared to control ( $n = 78$ ,  $i = 4$ ), similarly to the neonatal rat fibroblasts. In addition, 0.2 mM TC ( $n = 47$ ,  $i = 3$ ,  $p \leq 0.05$ ) had a significant depolarising effect on the human fetal fibroblasts. A, C) Depolarising effects of 0.2 mM TC were reversed by the presence of 1  $\mu$ M UDCA in fibroblasts from both species ( $n = 7$ ,  $i = 2$ ,  $p \leq 0.001$ ;  $n = 31$ ,  $i = 3$ ,  $p \leq 0.01$  respectively). In addition, the RMP of human fetal fibroblasts was further hyperpolarized by UDCA in the combined treatment in comparison to control ( $p \leq 0.01$ ). Acute incubation with  $K_{ATP}$  channel openers 30  $\mu$ M P1075 and 100  $\mu$ M pinacidil resulted in significant hyperpolarising shift of the resting membrane potential in both neonatal rat ( $n = 7$ ,  $i = 2$ ,  $p \leq 0.001$ ;  $n = 8$ ,  $i = 2$ ,  $p \leq 0.001$  respectively) and human fetal fibroblasts ( $n = 36$ ,  $i = 3$ ,  $p \leq 0.01$ ;  $n = 37$ ,  $i = 3$ ,  $p \leq 0.001$ ), although in the human fetal fibroblasts pinacidil was more potent compared to P1075 ( $p \leq 0.05$ ). D) Acute application of 20  $\mu$ M glibenclamide ( $n = 14$ ,  $i = 1$ ) did not induce significant changes in resting membrane potential of human fetal fibroblasts compared to matched controls ( $n = 14$ ,  $i = 1$ ). Subsequent incubation of 20  $\mu$ M glibenclamide with 1  $\mu$ M UDCA ( $n = 21$ ,  $i = 1$ ) prevented UDCA induced hyperpolarisation of human fetal fibroblasts, similar to neonatal rat fibroblasts (Miragoli et al., 2011a). The RMP of human fetal fibroblasts from this isolation was on average more negative than from previous isolations, potentially due to differences in genetic background or gestation. Additional recordings with 1  $\mu$ M UDCA showed that UDCA induced further hyperpolarisation also in these fibroblasts ( $n = 23$  cells,  $i = 1$ ,  $p \leq 0.01$ ).

of myofibroblast to fibroblast was first characterised by comparing the number of  $\alpha$ SMA-positive myofibroblasts in the total population of cells. Vimentin staining was used to confirm that  $\alpha$ SMA-negative cells were fibroblasts.

In neonatal rat fibroblasts, hypoxia treatment (24 h) led to a significantly increased number of  $\alpha$ SMA-positive cells ( $82.8\% \pm 4.3$ ;  $n = 34$ ,  $i = 3$ ) compared to normoxia ( $45.0\% \pm 3.3$ ;  $n = 69$ ,  $i = 3$ ,  $p \leq 0.001$ ) [Fig. 7A]. This was significantly reduced by UDCA treatment during hypoxia compared to hypoxia alone ( $43.0\% \pm 8.2$ ;  $n = 14$ ,  $i = 3$ ,  $p \leq 0.001$ ). 24 h treatment with 1  $\mu$ M UDCA did not induce significant changes in the number of  $\alpha$ SMA-positive cells in normoxia ( $38.7\% \pm 3.7$ ;  $n = 57$ ,  $i = 3$ ). Representative images of the effect of the various treatments on neonatal rat fibroblasts are

shown in Supplementary Fig. 3A.

In human fetal fibroblasts, a large percentage of cells were  $\alpha$ SMA-positive in normoxia ( $78.8\% \pm 4.2$ ;  $n = 34$ ,  $i = 3$ ) [Fig. 7C]. After hypoxia treatment (24 h), there was an increased number of  $\alpha$ SMA-positive cells, but this was not significant ( $95.9\% \pm 3.1$ ;  $n = 17$ ,  $i = 3$ ). 24 h treatment with 1  $\mu$ M UDCA led to a significant reduction in  $\alpha$ SMA-positive cells in both normoxia ( $59.7\% \pm 4.6$ ;  $n = 39$ ,  $i = 3$ ,  $p \leq 0.05$ ) and hypoxia ( $73.4\% \pm 4.8$ ;  $n = 45$ ,  $i = 3$ ,  $p \leq 0.05$ ). Representative images of the effect of the various treatments on human fetal fibroblasts are shown in Supplementary Fig. 3B.

Fibroblasts were relatively depolarised compared to the surrounding cardiomyocyte population, whilst UDCA induced

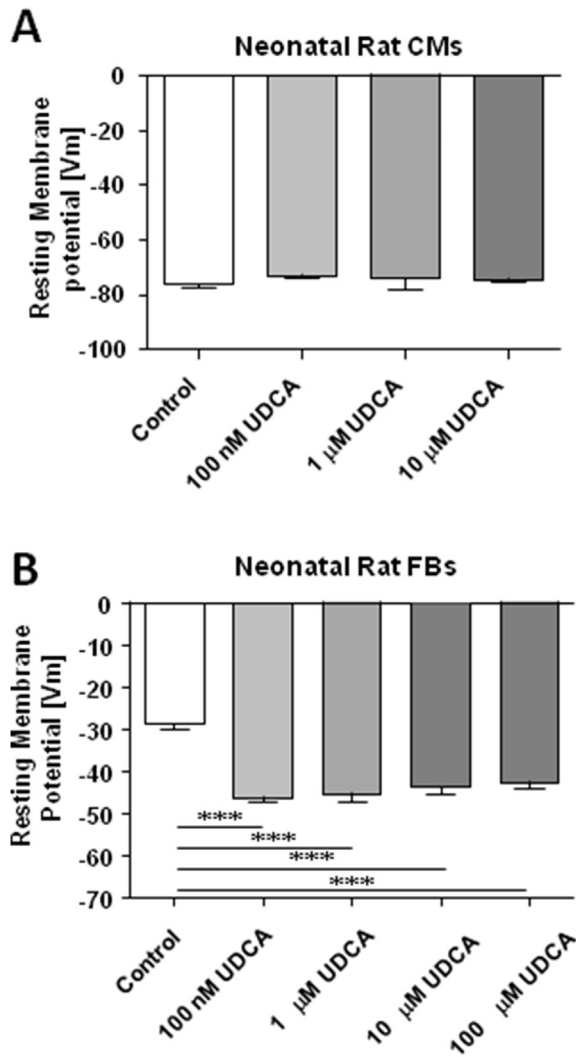


**Fig. 6. Chronic incubation with UDCA modulates membrane potential of neonatal rat fibroblasts, without affecting membrane potential of cardiomyocytes.** A) Chronic incubation with UDCA ranging from 100 nM to 10 μM (100 nM:  $n = 5$  cells,  $i = 2$  isolations; 1 μM:  $n = 4$ ,  $i = 2$ ; 10 μM:  $n = 6$ ,  $i = 2$ ) did not change resting membrane potential in neonatal rat cardiomyocytes compared to control ( $n = 36$ ;  $i = 2$ ). B) However, chronic incubation with UDCA induced hyperpolarisation in neonatal rat fibroblasts (100 nM:  $n = 8$ ,  $i = 2$ ; 1 μM:  $n = 4$ ,  $i = 2$ ; 10 μM:  $n = 4$ ,  $i = 2$ ; 100 μM:  $n = 4$ ,  $i = 2$ ) compared to control  $n = 40$ ,  $i = 2$ ,  $p \leq 0.001$ ).

hyperpolarisation of fibroblasts after acute treatment. Therefore we investigated whether hypoxia also induced RMP changes in neonatal rat fibroblasts [Fig. 8A] and human fetal fibroblasts [Fig. 8B]. 24 h treatment with hypoxia did not lead to significant changes in the RMP of neonatal rat fibroblasts ( $-16.3 \text{ mV} \pm 2.3$ ;  $n = 6$ ,  $i = 2$ ) compared to normoxia ( $-18.1 \text{ mV} \pm 1.7$ ;  $n = 30$ ,  $i = 3$ ) [Fig. 8A]. Acute 1 μM UDCA treatment induced significant hyperpolarisation in normoxia ( $-34.8 \text{ mV} \pm 3.9$ ;  $n = 28$ ,  $i = 3$ ,  $p \leq 0.01$ ) and in hypoxia ( $-28.1 \text{ mV} \pm 4.6$ ;  $n = 6$ ,  $i = 2$ ,  $p \leq 0.05$ ) compared to cells treated with normoxia or hypoxia alone.

In human fetal fibroblasts, 24 h treatment with hypoxia led to a significant decrease in RMP ( $-8.3 \text{ mV} \pm 1.2$ ;  $n = 12$ ,  $i = 3$ ,  $p \leq 0.05$ ) compared to normoxia ( $-22.5 \text{ mV} \pm 2.9$ ;  $n = 25$ ,  $i = 3$ ) [Fig. 8B]. On the other hand, acute treatment with 1 μM UDCA induced hyperpolarisation in cells pre-treated with normoxia ( $-41.0 \text{ mV} \pm 2.1$ ;  $n = 60$ ,  $i = 3$ ,  $p \leq 0.001$ ) or hypoxia ( $-22.7 \text{ mV} \pm 2.3$ ;  $n = 17$ ,  $i = 3$ ,  $p \leq 0.05$ ).

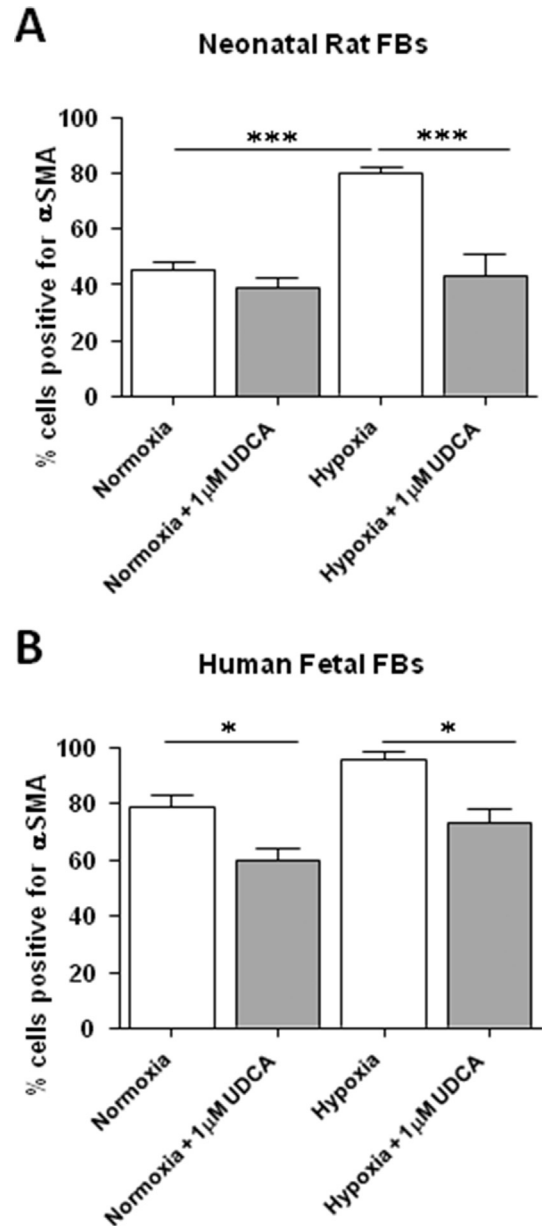


**Fig. 7. Effects of chronic hypoxia and UDCA incubation on αSMA expression in neonatal rat and human fetal fibroblasts.** A) Overnight hypoxia ( $n = 34$ ,  $i = 3$ ) induced an increase in the number of myofibroblasts, as seen by an increase in αSMA positive cells in neonatal rat fibroblasts compared to normoxia ( $n = 69$ ,  $i = 3$ ,  $p \leq 0.001$ ). The effect of hypoxia was attenuated by 1 μM UDCA treatment during the hypoxia ( $n = 14$ ,  $i = 3$ ,  $p \leq 0.001$ ). 1 μM UDCA treatment did not induce changes in the number of αSMA positive cells under normoxic conditions ( $n = 57$ ,  $i = 3$ ). B) There was a larger percentage of myofibroblasts in the human fetal fibroblast population even in normoxia ( $n = 34$ ,  $i = 3$ ). After hypoxia treatment (24 h) there was an increased number of αSMA-positive cells, but this was not significant ( $n = 17$ ,  $i = 3$ ). This number was reduced with overnight UDCA treatment in both normoxia ( $n = 39$ ,  $i = 3$ ,  $p \leq 0.05$ ) and hypoxia ( $73.4\% \pm 4.8$ ;  $n = 45$ ,  $i = 3$ ,  $p \leq 0.05$ ).

#### 4. Discussion

##### 4.1. Characterisation of the human fetal heart

For the first time, this study shows successful isolation of beating human fetal cardiomyocytes. The human fetal cardiomyocytes were characterised using immunofluorescence microscopy to visualise the expression and localisation of various

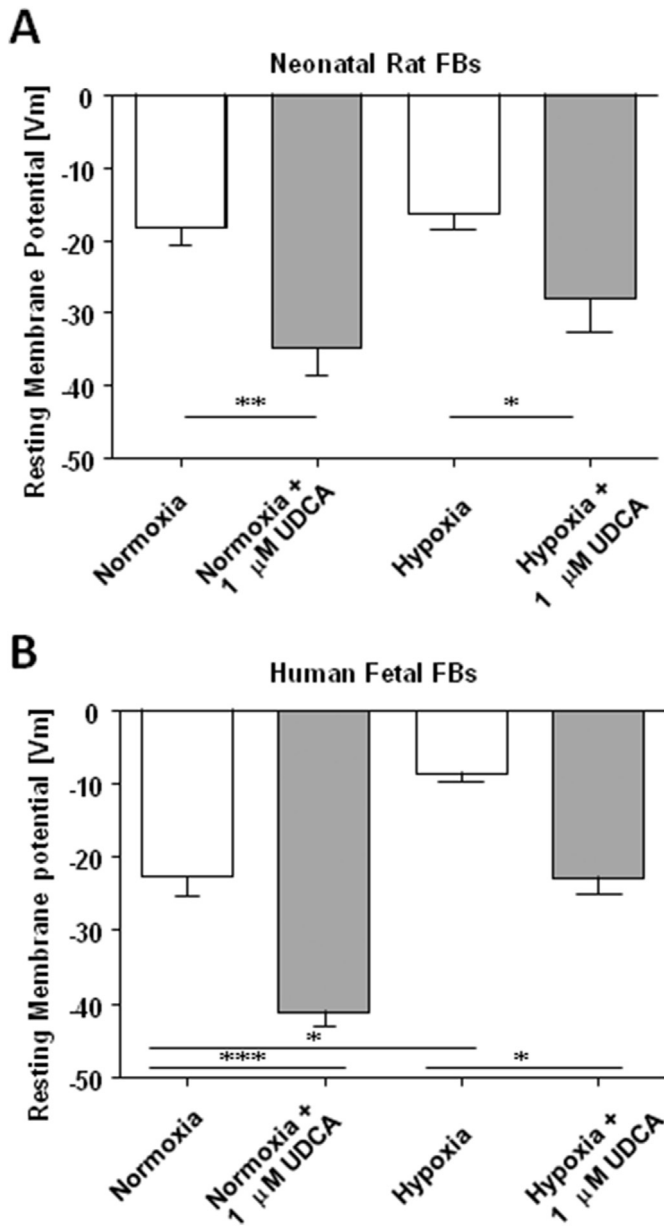


**Fig. 8. Resting membrane potential changes after chronic hypoxia in neonatal rat and human fetal fibroblasts.** A) Neonatal rat fibroblasts were treated for 24 h with hypoxia/normoxia and acutely with/without UDCA. Acute treatment with UDCA induced hyperpolarisation in neonatal rat fibroblasts after either normoxia ( $n = 28$ ,  $i = 3$ ,  $p \leq 0.01$ ) or hypoxia ( $n = 6$ ,  $i = 2$ ,  $p \leq 0.05$ ) compared to normoxia ( $n = 30$ ,  $i = 3$ ) or hypoxia alone ( $n = 6$ ,  $i = 2$ ). B) Human fetal fibroblasts were treated for 24 h with hypoxia/normoxia and acutely with/without UDCA. In human fetal fibroblasts, hypoxia induced significant depolarisation ( $n = 12$ ,  $i = 3$ ,  $p \leq 0.05$ ) compared to normoxia ( $n = 25$ ,  $i = 3$ ). This was attenuated by UDCA, inducing hyperpolarisation of the fibroblasts to normoxia levels ( $n = 17$ ,  $i = 3$ ,  $p \leq 0.05$  compared to hypoxia, ns compared to normoxia). In normoxia, UDCA ( $n = 60$ ,  $i = 3$ ,  $p \leq 0.001$ ) induced significant hyperpolarisation similar to results found in the neonatal rat fibroblasts (A) and (Miragoli et al., 2011a).

proteins known to be involved in the development and maturation of cardiomyocytes. The human fetal cardiomyocytes were compared to neonatal rat cardiomyocytes, which show similar localisation of  $\alpha$ -Actinin.

Connexin43 and  $\alpha$ -Actinin are essential proteins for the correct functioning of the contraction machinery of adult cardiomyocytes, as well as for signalling between cardiomyocytes. The expression

pattern of these proteins in rat neonatal cardiomyocytes and human fetal cardiomyocytes was very similar, as the cells showed an immature phenotype when compared to the adult 'organised' phenotype.

Scanning ion conductance microscopy analysis showed that there were similarities in the morphology and topography of the neonatal rat and human fetal cells. Neither neonatal rat nor human fetal cardiomyocytes show the well-structured crests or T-tubule structures within Z-grooves, which are distinctive features of adult cardiomyocytes (Gorelik et al., 2006b; Miragoli et al., 2011b; Nikolaev et al., 2010). The development of these structures occurs later on in gestation and continues after birth until cardiomyocytes reach full maturity. The development and maturation of T-tubules has been described in animal models (Al-Qusairi and Laporte, 2011; Chen et al., 2013; Seki, 2003). The development of the heart of a human neonate presumably occurs via similar processes though with a longer duration due to developmental differences in humans and rodents. In rodents, T-tubules develop during the first two weeks after birth, with rudimentary structures appearing by postnatal day 8. These structures show increased maturity, complexity and magnitude by postnatal day 14 (Seki, 2003; Ziman et al., 2010). There were striated patterns of  $\alpha$ -Actinin visible in the human fetal and neonatal rat cardiomyocytes, but possibly due to their shape, these patterns were not organised in the same manner as in adult cardiomyocytes, where they are perpendicular to the longitudinal axis of the cardiomyocytes (Maier et al., 2004). Instead the  $\alpha$ -Actinin staining appeared disordered following no discernible alignment. As these immature cells are not rod-shaped, unlike adult cardiomyocytes, the perpendicular line may not follow the shape of the cell and subsequent lines of  $\alpha$ -Actinin may not be arranged next to the lines closest to the membrane.

Connexin43 forms gap junctions between adult cardiomyocytes along the intercalated discs, which facilitate the inter-cellular exchange of molecules (Maier et al., 2004). In neonatal rat and human fetal cardiomyocytes cell morphology is not yet rod-shaped and therefore no clear intercalated discs can be identified. It is clear however, that Connexin43 is expressed in junctional areas between cells.

#### 4.2. The effect of UDCA on the heart

As UDCA is currently in use for clinical treatment of both ICP and other cardiac diseases (Geenes and Williamson, 2009; Geenes et al., 2014, 2013; Rainer et al., 2013; Von Haehling et al., 2012), the short term and long term effects of UDCA on neonatal cardiomyocytes and fibroblasts were investigated. Optical recording of calcium transients was carried out with control (HBSS) solution, followed by UDCA treatment (10 nM, 100 nM, 1  $\mu$ M or 100  $\mu$ M). No significant changes in calcium transient duration, time to peak or amplitude were seen at any of the concentrations tested, in either the cardiomyocyte only or co-culture models of neonatal rat cardiomyocytes co-cultured with fibroblasts. Similarly, neither acute nor chronic incubation with UDCA affected the resting membrane potential of neonatal rat cardiomyocytes at any of the concentrations used. UDCA induced significant hyperpolarisation in neonatal rat fibroblasts, similar to the acute effect shown in this study as well as previously (Miragoli et al., 2011a). Both studies suggest that UDCA is safe to use at the concentrations examined in neonatal rat cardiomyocytes and fibroblasts. This is of interest for clinical application as these concentrations are within the range of UDCA found to cross the placenta in ICP pregnancies treated with UDCA (Geenes et al., 2014). The total bile acid levels found to cross the placenta ranged from 2 to 10  $\mu$ mol/L in ICP pregnancies, with UDCA treatment reducing this total level significantly. In addition, UDCA was well-tolerated in patients with chronic heart failure (Sinisalo

et al., 1999; Tousoulis et al., 2012; Von Haehling et al., 2012).

#### 4.3. Counteracting the effect of taurocholic acid

The deleterious effect of high levels of TC on beating rate, amplitude, calcium transients, action potentials, and conduction velocity had previously been shown in neonatal rat cardiomyocytes and in the co-culture model of neonatal rat cardiomyocytes and fibroblasts (Gorelik et al., 2004, 2002; Kadir et al., 2010; Miragoli et al., 2011a; Williamson et al., 2001). Miragoli et al. (2011a) subsequently showed that UDCA can protect against the arrhythmic properties of TC, if incubated simultaneously with TC in the neonatal rat co-culture model (Miragoli et al., 2011a). Incubation with 0.5 mM TC alone led to conduction velocity slowing and formation of re-entry circuits in the co-culture model, which did not occur after co-incubation of 0.5 mM TC and 100 nM UDCA (Miragoli et al., 2011a). Conduction velocity was increased upon treatment with 100 nM UDCA together with 0.5 mM TC in the co-culture model, but did not change in the cardiomyocytes only model (Miragoli et al., 2011a). Here it was shown that even at lower concentrations there was an increase in action potential duration when the neonatal rat cardiomyocytes and fibroblasts were incubated with TC, providing evidence that TC has a similar effect to previously described effects, even at lower concentrations (Miragoli et al., 2011a).

We compared the effect of a lower concentration of TC on human fetal- and neonatal rat cardiomyocytes and fibroblasts. Increases in calcium transient duration, time to full calcium release and time for calcium reuptake in cardiomyocytes can have arrhythmogenic effects, as increased levels of  $Ca^{2+}$  in the cytoplasm can lead to a pro-arrhythmogenic state of the cell (Scoote and Williams, 2004). TC was shown to induce increased calcium transient duration and increased time to full release, which was attenuated by UDCA, indicating that UDCA may prevent TC-induced arrhythmias in neonatal rat cardiomyocytes cultured with fibroblasts. Optical recording of human fetal cardiomyocytes and fibroblasts was also carried out. These monolayers were grown in culture for a number of days, which allowed for the proliferation of residual fibroblasts. Human fetal cardiomyocytes with naturally occurring fibroblasts were also treated with the same concentration of TC (0.1 mM), but possibly due to an increased sensitivity the cells stopped beating and no fluorescence was detected after a shorter period of incubation than in the neonatal rat cardiomyocytes. UDCA prevented this reduction in fluorescence from occurring when incubated with TC, a potential protective effect. Further experiments should be carried out with a lower concentration of TC, to prevent early loss of cells due to the toxicity of TC. This difference between rodent and human cells may be due to species differences in sensitivity to bile acids. The use of lower concentrations of TC could further strengthen our hypothesis that arrhythmias in the fetus *in vivo* occur due to the toxicity of TC, even at low concentrations.

Both increases (tachycardia) and decreases in heart rate (bradycardia) can have fatal consequences for the fetus. A few studies have reported abnormal fetal heart rates ( $\leq 100$  or  $\geq 180$  beats per minute (bpm)), as well as reduced heart rate variability in ICP (Gorelik et al., 2003; Inizi et al., 2006; Laatikainen, 1975; Reid et al., 1976; Shand et al., 2008). Therefore, spontaneous beating rate was assessed in neonatal rat cardiomyocytes cultured with fibroblasts. There was a significant reduction in beating rate by almost 30% after TC treatment. Addition of UDCA led to a partial recovery to 80–90% of control. There was a significant improvement, although complete recovery was not obtained. This may be due to a slight physiological slowing in beating rate over time.

The fibroblast-driven arrhythmic effect is largely related to

direct depolarization of cardiomyocytes via gap junctional coupling, but a significant portion of this depolarization is induced by paracrine effects and by a tensile strain exerted by the myofibroblasts seeded on top of the cardiomyocytes (Thompson et al., 2011), and by the activation of cardiac fibroblast mechanosensitive channels (Grand et al., 2014). In spite of this multifactorial pro-arrhythmogenic aetiology, we observed that UDCA targeting  $K_{ATP}$  channels had minimal effects on cardiomyocytes only (these cells are already at their physiological RMP and the possible cellular input resistance remains unchanged after the administration of UDCA) but have a significant effect on myofibroblasts acting via the same  $K_{ATP}$  channels. The myofibroblast hyperpolarisation is therefore transferred to the coupled cardiomyocyte, reducing the overall RMP depolarization.

Whether arrhythmogenesis occurs *in vivo* depends on the degree of coupling, if heterocellular coupling occurs, and the density and the size of fibrotic areas, which are all prerequisites for eliciting ectopic activity *in vitro* and *in vivo* (Miragoli and Glukhov, 2015), regardless of the source-sink relationship on intracellular space (safety factor  $> 1$ ). We did not observe any effect of TC on cardiomyocyte RMP, but the effect is clearly present in cardiac fibroblasts of both human and rat origin [Fig. 4]. As we previously demonstrated TC alters calcium handling of cardiomyocytes via partial agonism of the muscarinic M2 receptors, this pro-arrhythmic pathway is activated by TC and does not affect cardiomyocyte RMP, therefore we may expect a synergistic effect with altered cardiac fibroblast RMP exerted by TC, when both cells are coupled (Kadir et al., 2010; Miragoli et al., 2011a). However, in this study, we did not investigate any downstream mechanisms for calcium release and uptake. We plan to focus on the role of Ryanodine receptors (particularly calcium sparks density, frequency and amplitude) and also on the role of SERCA2 in these cells, using new fluorophore technology (Wang et al., 2014).

One of the limitations of the present and previous studies is the relatively high concentration of TC used compared to what was recently shown to cross the placenta or accumulate in the fetus close to the time of delivery (Geenes et al., 2014). The total cholic acid levels ranged from 0.5 to 5  $\mu\text{mol/L}$ , of which TC ranged from 0.5 to 1.5  $\mu\text{mol/L}$  (Geenes et al., 2014). As there may be a cumulative effect of the bile acid exposure over a long period of time in the fetus, which has not been replicated in the neonatal rat models, this higher dose was chosen to simulate maternal serum bile acid levels. Hence it may still provide valuable information with regards to the effects of TC on cardiomyocytes and fibroblasts. If further samples become available, we will expand this work with lower concentrations of TC, to ensure the cells are not exposed to such a toxic load.

#### 4.4. UDCA alters membrane potential and modulates fibroblast structure

The number of myofibroblasts in neonatal rat and human fetal fibroblast populations were compared. An increased number of  $\alpha\text{SMA}$ -positive human fetal fibroblasts were found even under control conditions, which may suggest that effects of a hypoxic environment *in utero* still persisted under short-term culture conditions (less than 1 month). Upon treatment with hypoxia, this number further increased and in addition, hypoxia induced significant depolarisation in these human fetal fibroblasts. This suggests that the natural 'contamination' seen in the human fetal cardiomyocyte culture is similar to the gestational appearance of myofibroblasts during the development of the human fetal heart, and that it is comparable to the neonatal rat co-cultures described here and previously (Miragoli et al., 2011a). Interestingly, UDCA treatment led to a reduction in the number of myofibroblasts. This

is similar to the effect of UDCA on liver fibrosis (Fickert et al., 2006; Halilbasic et al., 2009).

Since the fetus develops in partial hypoxia, the effect of hypoxia and 1  $\mu\text{M}$  UDCA on RMP was investigated (Chilton et al., 2005; Webster and Abela, 2007). Hypoxia induced a relative depolarisation in both neonatal rat and human fetal fibroblasts, although this was only found to be significant in human fetal fibroblasts.

One previous study examined the ionic basis of membrane potential and associated changes in physiological function of both rat fibroblasts and myofibroblasts (Chilton et al., 2005). Hyperpolarisation of fibroblasts is associated with cell proliferation and/or survival, while depolarisation had no effect (Chilton et al., 2005). On the other hand, depolarisation would be expected to result in fibroblast contraction, which can be measured by collagen deformation assays. In the present study we report that hypoxia-induced depolarisation of human fetal fibroblasts positively correlates with  $\alpha\text{SMA}$  expression, which is linked to conversion of fibroblasts to myofibroblasts. It is already established that mechanical forces to which fibroblasts are exposed can influence their physiological function, by putatively changing their membrane potential. Equally, hypoxic/ischaemic environments can cause down-regulation of ion channels involved in maintaining RMP (Benamer et al., 2013, 2009). In our study we saw a significant positive shift of membrane potential in human fetal fibroblasts [Fig. 8B], which is indicative of channel subunit reduction. This is plausible given that hypoxia treatment was applied overnight.

Acute treatment with 1  $\mu\text{M}$  UDCA led to significant hyperpolarisation of the hypoxia-treated neonatal rat and human fetal fibroblasts. Similar results were obtained under normoxic conditions with 1  $\mu\text{M}$  UDCA. To further evaluate potential molecular targets responsible for the UDCA-mediated negative shift (hyperpolarisation) in membrane potential observed in human fetal fibroblasts, selective  $\text{K}_{\text{ATP}}$  channel agents were employed (Lange et al., 2002). Addition of  $\text{K}_{\text{ATP}}$  channel agonists induces efflux of  $\text{K}^+$  from the cells, lowering the membrane potential to more negative values (Chilton et al., 2005; Lange et al., 2002; Shibukawa et al., 2005). It was shown previously that treatment with the  $\text{K}_{\text{ATP}}$  channel blocker glibenclamide prevented UDCA induced hyperpolarisation of RMP in neonatal rat fibroblasts (Miragoli et al., 2011a). The present study shows that glibenclamide does not induce significant changes in the RMP of human fetal fibroblasts, and as in neonatal rat fibroblasts, prevents UDCA induced hyperpolarisation [Fig. 5D]. As the effect of UDCA on RMP is similar to that of two  $\text{K}_{\text{ATP}}$  channel agonists, pinacidil and its analogue P1075, and is blocked by glibenclamide,  $\text{K}_{\text{ATP}}$  channels are likely to be the main target of UDCA. In addition, changes in RMP seen with UDCA were obtained following short-term incubation, suggesting that an effect on channel function, rather than on expression is associated with these changes. It would be interesting to further examine whether UDCA has an effect on whole-cell  $\text{K}_{\text{ATP}}$  current.

Although contribution of other  $\text{K}^+$  channels subtypes in UDCA-mediated alteration of fibroblast potential across the cell have to be taken into account, only  $\text{K}^+$  channels are able to mediate RMP. For instance, inwardly rectifying  $\text{K}^+$  ( $\text{K}_{\text{ir}}$ ) channels are thought to be the principal  $\text{K}^+$  channel subtype responsible for maintaining RMP (Baczko et al., 2003). Chilton et al. (2005) reported  $\text{K}^+$  conductance in adult rat cardiac myofibroblasts to be carried by several  $\text{K}^+$  channel subtypes, namely  $\text{K}_{\text{ir}}$  and delayed rectifier voltage-gated  $\text{K}^+$  ( $\text{K}_{\text{v}}$ ) (Chilton et al., 2005; Shibukawa et al., 2005). They recorded two types of currents carried by  $\text{K}_{\text{ir}}$  channels, one active near the RMP (inward), and a second, time- and voltage-dependent current at potentials positive to  $-40$  mV (outward) (Chilton et al., 2005; Shibukawa et al., 2005). mRNA transcripts corresponding to Kir2.1 and Kir6.1 subtypes were detected, the latter encodes a pore-forming  $\text{K}_{\text{ATP}}$  subunit, which most likely carries time- and

voltage-dependent outward  $\text{K}^+$  current (Chilton et al., 2005). Although further investigation is necessary, these data suggest that membrane potential in human fetal fibroblasts is partially mediated by  $\text{K}_{\text{ATP}}$  channels, which belong to the  $\text{K}_{\text{ir}}$  channel family and which can be modulated by UDCA, a molecule with fibroblast-specific, anti-arrhythmic properties (Miragoli et al., 2011a). Apart from their role in maintaining the membrane potential, these channels could be responsible for modulating the threshold for cellular excitability (crucial in cardiomyocyte-fibroblasts coupling), and could contribute to  $\text{K}^+$  homeostasis in cardiac tissue (Ruppersberg, 2000).

## 5. Conclusions

In conclusion, we show that human fetal cardiomyocytes have similar characteristics to neonatal rat cardiomyocytes, both in localisation of cardiac markers, cellular topography and calcium transient parameters. The effect of TC was investigated in both the neonatal rat model of cardiomyocytes and fibroblasts and the human fetal model using human fetal cardiomyocytes with interspersed, naturally occurring fibroblasts. The prolongation of calcium transient duration induced by TC in both models was attenuated by UDCA. In the neonatal model UDCA, also prevented potentially arrhythmic changes in action potential duration and beating rate. To further investigate the effect of bile acids on fibroblasts, RMP recordings were carried out. TC depolarised both neonatal rat and human fetal fibroblasts, but had no effect on neonatal rat cardiomyocyte membrane potential. UDCA hyperpolarised fibroblasts, and prevented TC-induced depolarization. Furthermore, UDCA induced hyperpolarisation of both neonatal rat and human fetal fibroblasts when cultured in hypoxia for 24 h. UDCA treatment also led to a reduced number of human fetal myofibroblasts in both normoxia and hypoxia. Our study thereby provides further evidence of the protective effect of UDCA on the human fetal heart. This could be important in validating UDCA as an antifibrotic and antiarrhythmic drug for treatment of fetal arrhythmia in ICP, as well as treatment of adult heart failure.

## Funding

This study was funded by a BBSRC PhD Studentship (FS). The research was also supported by Heart Research UK (TRP10/13) and by the National Institute for Health Research (NIHR) Biomedical Research Centres based at Guy's and St Thomas' NHS Foundation Trust and at Imperial College Healthcare NHS Trust. The views expressed are those of the author(s) and not necessarily those of the NHS, the NIHR or the Department of Health. The human fetal heart tissue was obtained as a sub-collection of the Imperial College Tissue Bank. The funders had no role in study design, data collection and analysis, decision to publish, or preparation of the manuscript.

## Acknowledgements

We thank Dagmar Tapon and Professor Phillip Bennett for the help with obtaining the human fetal samples. We are grateful for the permission from the Imperial College Tissue Bank for obtaining this tissue. We are grateful to Dr. Jennifer Simonotto for the generation of the Matlab code used to analyse the optical recording data.

## Appendix A. Supplementary data

Supplementary data related to this article can be found at <http://dx.doi.org/10.1016/j.pbiomolbio.2016.01.003>.

## References

- Al-Qusairi, L., Laporte, J., 2011. T-tubule biogenesis and triad formation in skeletal muscle and implication in human diseases. *Skelet. Muscle* 1, 26. <http://dx.doi.org/10.1186/2044-5040-1-26>.
- Baczkó, L., Giles, W.R., Light, P.E., 2003. Resting membrane potential regulates Na(+)-Ca2+ exchange-mediated Ca2+ overload during hypoxia-reoxygenation in rat ventricular myocytes. *J. Physiol.* 550, 889–898. <http://dx.doi.org/10.1113/jphysiol.2003.043372>.
- Banerjee, I., Fuseler, J.W., Price, R.L., Borg, T.K., Baudino, T.A., 2007. Determination of cell types and numbers during cardiac development in the neonatal and adult rat and mouse. *Am. J. Physiol. Heart Circ. Physiol.* 293, H1883–H1891. <http://dx.doi.org/10.1152/ajpheart.00514.2007>.
- Benamer, N., Maati, H.M.O., Demolombe, S., Cantereau, A., Delwail, A., Bois, P., Bescond, J., Faviere, J.-F.F., Moha Ou Maati, H., Demolombe, S., Cantereau, A., Delwail, A., Bois, P., Bescond, J., Faviere, J.-F.F., Maati, H.M.O., Demolombe, S., Cantereau, A., Delwail, A., Bois, P., Bescond, J., Faviere, J.-F.F., 2009. Molecular and functional characterization of a new potassium conductance in mouse ventricular fibroblasts. *J. Mol. Cell. Cardiol.* 46, 508–517. <http://dx.doi.org/10.1016/j.yjmcc.2008.12.016>.
- Benamer, N., Vasquez, C., Mahoney, V.M., Steinhardt, M.J., Coetzee, W.A., Morley, G.E., 2013. Fibroblast KATP currents modulate myocyte electrophysiology in infarcted hearts. *Am. J. Physiol. Circ. Physiol.* 304, H1231–H1239. <http://dx.doi.org/10.1152/ajpheart.00878.2012>.
- Chen, B., Guo, A., Zhang, C., Chen, R., Zhu, Y., Hong, J., Kutschke, W., Zimmerman, K., Weiss, R.M., Zingman, L., Anderson, M.E., Wehrens, X.H.T., Song, L.-S., 2013. Critical roles of junctophilin-2 in T-tubule and excitation-contraction coupling maturation during postnatal development. *Cardiovasc. Res.* 100, 54–62. <http://dx.doi.org/10.1093/cvr/cvt180>.
- Chilton, L., Ohya, S., Freed, D., George, E., Drobic, V., Shibukawa, Y., Maccannell, K.A., Imaizumi, Y., Clark, R.B., Dixon, I.M.C., Giles, W.R., 2005. K+ currents regulate the resting membrane potential, proliferation, and contractile responses in ventricular fibroblasts and myofibroblasts. *Am. J. Physiol. Circ. Physiol.* 288, H2931–H2939. <http://dx.doi.org/10.1152/ajpheart.01220.2004>.
- Clancy, R.M., Zheng, P., O'Mahony, M., Izmirly, P., Zavadil, J., Gardner, L., Buyon, J.P., 2007. Role of hypoxia and cAMP in the transdifferentiation of human fetal cardiac fibroblasts: implications for progression to scarring in autoimmune-associated congenital heart block. *Arthritis Rheum.* 56, 4120–4131. <http://dx.doi.org/10.1002/art.23061>.
- Fickert, P., Wagner, M., Marschall, H.-U.H., Fuchsbichler, A., Zollner, G., Tsybrovskyy, O., Zatloukal, K., Liu, J., Waalkes, M.P., Cover, C., Denk, H., Hofmann, A.F., Jaeschke, H., Trauner, M., 2006. 24-norUrsodeoxycholic acid is Superior to ursodeoxycholic acid in the treatment of sclerosing cholangitis in Mdr2 (Abcb4) knockout mice. *Gastroenterology* 130, 465–481. <http://dx.doi.org/10.1053/j.gastro.2005.10.018>.
- Inizi, S.A.I., Gupta, R., Gale, A., Al Inizi, S., Gupta, R., Gale, A., 2006. Fetal tachyarrhythmia with atrial flutter in obstetric cholestasis. *Int. J. Gynecol. Obstet.* 93, 53–54. <http://dx.doi.org/10.1016/j.ijgo.2005.12.030>.
- Geenes, V., Williamson, C., 2009. Intrahepatic cholestasis of pregnancy. *World J. Gastroenterol.* 15, 2049. <http://dx.doi.org/10.3748/wjg.15.2049>.
- Geenes, V., Chappell, L.C., Seed, P.T., Steer, P.J., Knight, M., Williamson, C., 2013. Association of severe intrahepatic cholestasis of pregnancy with adverse pregnancy outcomes: a prospective population-based case-control study. *Hepatology* 1–10. <http://dx.doi.org/10.1002/hep.26617>.
- Geenes, V., Lövgren-Sandblom, A., Benthin, L., Lawrence, D., Chambers, J., Gurung, V., Thornton, J., Chappell, L., Khan, E., Dixon, P., Marschall, H.-U.U., Williamson, C., Lövgren-Sandblom, A., Benthin, L., Lawrence, D., Chambers, J., Gurung, V., Thornton, J., Chappell, L., Khan, E., Dixon, P., Marschall, H.-U.U., Williamson, C., 2014. The reversed fetomaternal bile acid gradient in intrahepatic cholestasis of pregnancy is corrected by ursodeoxycholic acid. *PLoS One* 9, e83828. <http://dx.doi.org/10.1371/journal.pone.0083828>.
- Glantz, A., Marschall, H.-U.U., Mattsson, L.-A.A., 2004. Intrahepatic cholestasis of pregnancy: relationships between bile acid levels and fetal complication rates. *Hepatology* 40, 467–474. <http://dx.doi.org/10.1002/hep.20336>.
- Gorelik, J., Harding, S.E., Shevchuk, A.I., Korallage, D., Lab, M., de Swiet, M., Korchev, Y., Williamson, C., 2002. Taurocholate induces changes in rat cardiomyocyte contraction and calcium dynamics. *Clin. Sci. (Lond.)* 103, 191–200. <http://dx.doi.org/10.1042/>.
- Gorelik, J., Shevchuk, A.I., Diakonov, I., de Swiet, M., Lab, M., Korchev, Y., Williamson, C., Gorelik, J., Shevchuk, A.I., Diakonov, I., de Swiet, M., Lab, M., Korchev, Y., W, C., 2003. Dexamethasone and ursodeoxycholic acid protect against the arrhythmogenic effect of taurocholate in an *in vitro* study of rat cardiomyocytes. *BJOG Int. J. Obstet. Gynaecol.* 110, 424–429. [http://dx.doi.org/10.1016/S1470-0328\(03\)02973-2](http://dx.doi.org/10.1016/S1470-0328(03)02973-2).
- Gorelik, J., Shevchuk, A., de Swiet, M., Lab, M., Korchev, Y., Williamson, C., 2004. Comparison of the arrhythmogenic effects of tauro- and glycoconjugates of cholic acid in an *in vitro* study of rat cardiomyocytes. *BJOG Int. J. Obstet. Gynaecol.* 111, 867–870. <http://dx.doi.org/10.1111/j.1471-0528.2004.00166.x>.
- Gorelik, J., Patel, P., Ng'andwe, C., Vodyanov, I., Diakonov, I., Lab, M., Korchev, Y., Williamson, C., 2006a. Genes encoding bile acid, phospholipid and anion transporters are expressed in a human fetal cardiomyocyte culture. *BJOG* 113, 552–558. <http://dx.doi.org/10.1111/j.1471-0528.2006.00918.x>.
- Gorelik, J., Yang, L.Q., Zhang, Y., Lab, M., Korchev, Y., Harding, S.E., 2006b. A novel Z-groove index characterizing myocardial surface structure. *Cardiovasc. Res.* 72, 422–429. <http://dx.doi.org/10.1016/j.cardiores.2006.09.009>.
- Gorelik, J., Wright, P.T., Lyon, A.R., Harding, S.E., 2013. Spatial control of the  $\beta$ AR system in heart failure: the transverse tubule and beyond. *Cardiovasc. Res.* 98, 216–224. <http://dx.doi.org/10.1093/cvr/cvt005>.
- Grand, T., Salvarani, N., Jousset, F., Rohr, S., 2014. Aggravation of cardiac myofibroblast arrhythmogenicity by mechanical stress. *Cardiovasc. Res.* 104, 489–500. <http://dx.doi.org/10.1093/cvr/cvt227>.
- Halilbasic, E., Fiorotto, R., Fickert, P., Marschall, H.-U., Moustafa, T., Spirli, C., Fuchsbichler, A., Gumhold, J., Silbert, D., Zatloukal, K., Langner, C., Maitra, U., Denk, H., Hofmann, A.F., Strazzabosco, M., Trauner, M., 2009. Side chain structure determines unique physiologic and therapeutic properties of nor-ursodeoxycholic acid in Mdr2<sup>-/-</sup> mice. *Hepatology* 49, 1972–1981. <http://dx.doi.org/10.1002/hep.22891>.
- Kadir, S.H.S.A., Miragoli, M., Abu-Hayyeh, S., Moshkov, A.V., Xie, Q., Keitel, V., Nikolaev, V.O., Williamson, C., Gorelik, J., 2010. Bile acid-induced arrhythmia is mediated by muscarinic M2 receptors in neonatal rat cardiomyocytes. *PLoS One* 5, e9689.
- Laatikainen, T.J., 1975. Fetal bile acid levels in pregnancies complicated by maternal intrahepatic cholestasis. *Am. J. Obstet. Gynecol.* 122, 852–856.
- Lange, U., Löffler-Walz, C., Englert, H.C., Hambrock, A., Russ, U., Quast, U., 2002. The stereoantagonists of a pinacidil analog open or close cloned ATP-sensitive K<sup>+</sup> channels. *J. Biol. Chem.* 277, 40196–40205. <http://dx.doi.org/10.1074/jbc.M206685200>.
- Lyon, A.R., MacLeod, K.T., Zhang, Y., Garcia, E., Kanda, G.K., Lab, M.J., Korchev, Y.E., Harding, S.E., Gorelik, J., 2009. Loss of T-tubules and other changes to surface topography in ventricular myocytes from failing human and rat heart. *Proc. Natl. Acad. Sci. U. S. A.* 106, 6854–6859. <http://dx.doi.org/10.1073/pnas.0809777106>.
- Maier, S.K.G., Westenbroek, R.E., McCormick, K.A., Curtis, R., Scheuer, T., Catterall, W.A., 2004. Distinct subcellular localization of different sodium channel  $\alpha$  and  $\beta$  subunits in single ventricular myocytes from mouse heart. *Circulation* 109, 1421–1427. <http://dx.doi.org/10.1161/01.CIR.0000121421.61896.24>.
- Mays, J.K., 2010. The active management of intrahepatic cholestasis of pregnancy. *Curr. Opin. Obstet. Gynecol.* 22, 100–103. <http://dx.doi.org/10.1097/GCO.0b013e328337238d>.
- Miragoli, M., Glukhov, A.V., 2015. Atrial fibrillation and fibrosis: beyond the cardiomyocyte centric view. *Biomed. Res. Int.* 2015, 798768. <http://dx.doi.org/10.1155/2015/798768>.
- Miragoli, M., Kadir, S.H.S.A., Sheppard, M.N., Salvarani, N., Virta, M., Wells, S., Lab, M.J., Nikolaev, V.O., Moshkov, A., Hague, W.M., Rohr, S., Williamson, C., Gorelik, J., 2011a. A protective antiarrhythmic role of ursodeoxycholic acid in an *in vitro* rat model of the cholestatic fetal heart. *Hepatology* 54, 1282–1292. <http://dx.doi.org/10.1002/hep.24492>.
- Miragoli, M., Moshkov, A., Novak, P., Shevchuk, A., Nikolaev, V.O., El-Hamamsy, I., Potter, C.M.F., Wright, P., Kadir, S.H.S.A., Lyon, A.R., Mitchell, J.A., Chester, A.H., Klenerman, D., Lab, M.J., Korchev, Y.E., Harding, S.E., Gorelik, J., 2011b. Scanning ion conductance microscopy: a convergent high-resolution technology for multi-parametric analysis of living cardiovascular cells. *J. R. Soc. Interface* 8, 913–925. <http://dx.doi.org/10.1098/rsif.2010.0597>.
- Nikolaev, V.O., Moshkov, A., Lyon, A.R., Miragoli, M., Novak, P., Paur, H., Lohse, M.J., Korchev, Y.E., Harding, S.E., Gorelik, J., 2010. Beta2-adrenergic receptor redistribution in heart failure changes cAMP compartmentation. *Science* 327, 1653–1657. <http://dx.doi.org/10.1126/science.1185988>.
- Patterson, A.J., Zhang, L., 2010. Hypoxia and fetal heart development. *Curr. Mol. Med.* 10, 653–666.
- Rainer, P.P., Primessing, U., Harenkamp, S., Doleschal, B., Wallner, M., Fauler, G., Stojakovic, T., Wachter, R., Yates, A., Groschner, K., Trauner, M., Pieske, B.M., von Lewinski, D., 2013. Bile acids induce arrhythmias in human atrial myocardium—implications for altered serum bile acid composition in patients with atrial fibrillation. *Heart* 99, 1685–1692. <http://dx.doi.org/10.1136/heartjnl-2013-304163>.
- Reid, R., Ivey, K.J., Rencoret, R.H., Storey, B., 1976. Fetal complications of obstetric cholestasis. *Br. Med. J.* 1, 870–872.
- Ruppertsberg, J.P., 2000. Intracellular regulation of inward rectifier K<sup>+</sup> channels. *Pflügers Arch.* 441, 1–11.
- Scoote, M., Williams, A.J., 2004. Myocardial calcium signalling and arrhythmia pathogenesis. *Biochem. Biophys. Res. Commun.* 322, 1286–1309. <http://dx.doi.org/10.1016/j.bbrc.2004.08.034>.
- Seki, S., 2003. Fetal and postnatal development of Ca<sup>2+</sup> transients and Ca<sup>2+</sup> sparks in rat cardiomyocytes. *Cardiovasc. Res.* 58, 535–548. [http://dx.doi.org/10.1016/S0008-6363\(03\)00255-4](http://dx.doi.org/10.1016/S0008-6363(03)00255-4).
- Sepúlveda, W.H., González, C., Cruz, M.A., Rudolph, M.I., 1991. Vasoconstrictive effect of bile acids on isolated human placental chorionic veins. *Eur. J. Obstet. Gynecol. Reprod. Biol.* 42, 211–215.
- Shand, A.W., Dickinson, J.E., D'Orsogna, L., 2008. Refractory fetal supraventricular tachycardia and obstetric cholestasis. *Fetal Diagn. Ther.* 24, 277–281. <http://dx.doi.org/10.1159/000151676>.
- Sheikh Abdul Kadir, S.H., Miragoli, M., Abu-Hayyeh, S., Moshkov, A.V., Xie, Q., Keitel, V., Nikolaev, V.O., Williamson, C., Gorelik, J., Kadir, S.H.S.A., Miragoli, M., Abu-Hayyeh, S., Moshkov, A.V., Xie, Q., Keitel, V., Nikolaev, V.O., Williamson, C., Gorelik, J., 2010. Bile acid-induced arrhythmia is mediated by muscarinic M2 receptors in neonatal rat cardiomyocytes. *PLoS One* 5, e9689. <http://dx.doi.org/10.1371/journal.pone.0009689>.
- Shibukawa, Y., Chilton, E.L., Maccannell, K.A., Clark, R.B., Giles, W.R., 2005. K+

- currents activated by depolarization in cardiac fibroblasts. *Biophys. J.* 88, 3924–3935. <http://dx.doi.org/10.1529/biophysj.104.054429>.
- Sinisalo, J., Vanhanen, H., Pajunen, P., Vapaatalo, H., Nieminen, M.S., 1999. Ursodeoxycholic acid and endothelial-dependent, nitric oxide-independent vasodilatation of forearm resistance arteries in patients with coronary heart disease. *Br. J. Clin. Pharmacol.* 47, 661–665.
- Thompson, S.A., Copeland, C.R., Reich, D.H., Tung, L., 2011. Mechanical coupling between myofibroblasts and cardiomyocytes slows electric conduction in fibrotic cell monolayers. *Circulation* 123, 2083–2093.
- Tousoulis, D., Papageorgiou, N., Stefanadis, C., 2012. Ursodeoxycholic acid in patients with chronic heart failure. *J. Am. Coll. Cardiol.* 60, 1579–1580. <http://dx.doi.org/10.1016/j.jacc.2012.02.089>.
- Von Haehling, S., Schefold, J.C., Jankowska, E.A., Springer, J., Vazir, A., Kalra, P.R., Sandek, A., Fauler, G.G., Stojakovic, T., Trauner, M., Ponikowski, P., Volk, H.-D.D., Doehner, W., Coats, A.J.S., Poole-Wilson, P.A., Anker, S.D., 2012. Ursodeoxycholic acid in patients with chronic heart failure: a double-blind, randomized, placebo-controlled, crossover trial. *J. Am. Coll. Cardiol.* 59, 585–592. <http://dx.doi.org/10.1016/j.jacc.2011.10.880>.
- Walsh, K.B., Zhang, J., 2008. Neonatal rat cardiac fibroblasts express three types of voltage-gated K<sup>+</sup> channels: regulation of a transient outward current by protein kinase C. *Am. J. Physiol. Heart Circ. Physiol.* 294, H1010–H1017. <http://dx.doi.org/10.1152/ajpheart.01195.2007>.
- Wang, L., Myles, R.C., De Jesus, N.M., Ohlendorf, A.K.P., Bers, D.M., Ripplinger, C.M., 2014. Optical mapping of sarcoplasmic reticulum Ca<sup>2+</sup> in the intact heart: ryanodine receptor refractoriness during alternans and fibrillation. *Circ. Res.* 114, 1410–1421. <http://dx.doi.org/10.1161/CIRCRESAHA.114.302505>.
- Webster, W.S., Abela, D., 2007. The effect of hypoxia in development. *Birth Defects Res. C Embryo Today Rev.* 81, 215–228. <http://dx.doi.org/10.1002/bdrc.20102>.
- Williamson, C., Gorelik, J., Eaton, B.M., Lab, M., de Swiet, M., Korchev, Y., 2001. The bile acid taurocholate impairs rat cardiomyocyte function: a proposed mechanism for intra-uterine fetal death in obstetric cholestasis. *Clin. Sci. (Lond.)* 100, 363–369.
- Ziman, A.P., Gómez-Viquez, N.L., Bloch, R.J., Lederer, W.J., 2010. Excitation-contraction coupling changes during postnatal cardiac development. *J. Mol. Cell. Cardiol.* 48, 379–386. <http://dx.doi.org/10.1016/j.yjmcc.2009.09.016>.